Stack, J. R., Gottfried, M. D., & Stocker, M. R. (2025). A new Lower Permian ray-finned fish (Actinopterygii) from South Dakota and the use of tree space to find rogue taxa in phylogenetic analysis of morphological data. *Bulletin of the Society of Systematic Biologists*. https://doi.org/10.18061/bssb.v3i2.9825

Investigations

A New Lower Permian Ray-Finned Fish (Actinopterygii) From South Dakota and the Use of Tree Space to Find Rogue Taxa in Phylogenetic Analysis of Morphological Data

Jack R. Stack[1], Michael D. Gottfried[2], Michelle R. Stocker[1]

[1] Department of Geological Sciences, Virginia Tech, [2] Earth and Environmental Sciences, Michigan State University

https://doi.org/10.18061/bssb.v3i2.9825

Bulletin of the Society of Systematic Biologists

Abstract

The ray-finned fishes (Actinopterygii) include one out of two species of vertebrate on Earth today. The mineralized skeletons of ray-finned fishes are a common component of the vertebrate fossil record extending back 380 million years, providing a window into the history of actinopterygian diversification. The divergence of extant lineages from the "palaeoniscoids", a grade of Paleozoic and early Mesozoic Era species, remains unresolved in analyses of morphological data despite more than four decades of phylogenetic research. We describe a new ray-finned fish, *Tenupiscis dakotaensis* gen et. sp. nov., from the Lower Permian (Kungurian) of South Dakota to strengthen our phylogenetic knowledge of Mississippian–Triassic actinopterygians. Our initial parsimony and Bayesian phylogenetic analyses were unable to resolve the relationships of Mississippian–Triassic "palaeoniscoids". We analyzed the topological variation among the trees sampled in each phylogenetic search (tree space) to determine if uncertainty was concentrated in a small subset of species with highly uncertain phylogenetic relationships relative to other terminal taxa (rogue taxa) or distributed evenly amongst early actinopterygians. The relationships of fourteen species were unresolved in the parsimony strict consensus due to a single rogue taxon ("*Kalops monophyrum*"). Parsimony and Bayesian analyses with the rogue pruned or recoded find the initially unresolved Mississippian–Triassic "palaeoniscoids" (including *Tenupiscis*) branching from the actinopterygian stem or from the base of pan-Neopterygii. Our work supports the emerging consensus that Paleozoic Era ray-finned fishes include clades of stem actinopterygians and the earliest members of the actinopterygian crown group. We also demonstrate an approach to identifying and mitigating rogue taxon effects in phylogenetic analysis of morphological data from new fossil taxa.

Introduction

Synthesis

In the age of phenomics (Houle et al., 2010) morphological datasets ranging across many species (i.e., the effort to scan every species of ray-finned fish; Summers, 2018) linked with phylogenetic knowledge can illuminate macroevolution on an unprecedented scale. Integrating such data with information from the fossil record is critical for reliably estimating the tempo of evolution (Heath et al., 2014; Lee & Palci, 2015; Wright et al., 2022), providing context for the evolution of traits in extant species (Corn et al., 2022), and improving model selection of trait evolution in phylogenetic comparative methods (Liow et al., 2023; Louca & Pennell, 2020; Slater et al., 2012). However, extinct species can have highly uncertain or unstable phylogenetic positions relative to other terminal taxa (rogue, wildcard, unstable, or floating taxa; Nixon & Wheeler, 1992; Sanderson & Shaffer, 2002; Trautwein et al., 2011; Wilkinson, 2003; Wilkinson & Benton, 1995). We analyze the phylogenetic position of a new late Paleozoic actinopterygian as an empirical case study of how novel "tree space" methods can illuminate rogue taxa as sources of uncertainty in phylogenetic analyses of morphological data (Hillis et al., 2005; Smith, 2022; Wright & Lloyd, 2020). This study shows how future researchers can reliably search for rogue taxa and demonstrate effective methods for alleviating rogue taxon effects.

The ray-finned fishes (Actinopterygii) are the most diverse and speciose group of vertebrates on Earth (Nelson et al., 2016). Although molecular clock studies indicate that

the actinopterygian crown group arose in the Mississippian Period (~359–323 Ma; Cohen et al., 2013), the earliest unambiguous fossils of crown group ray-finned fishes are known from the Early Triassic, some ~72 million years later (Faircloth et al., 2013; Hurley et al., 2007; Near et al., 2012; Romano, 2021). The intervening chronological gap holds a plethora of morphologically diverse extinct species of "palaeoniscoid" actinopterygians (i.e., "paleopterygians", "palaeoniscids"; Regan, 1923), which has been recognized as paraphyletic since the initial application of cladistic methods to paleoicthyology (Gardiner, 1984; Gardiner & Schaeffer, 1989; Patterson, 1982). The relationships of "palaeoniscoids" are a longstanding and unyielding problem in paleoichthyology (e.g., Berg, 1947; Coates, 1993; Gardiner, 1984; Gardiner & Schaeffer, 1989; Giles et al., 2017; Patterson, 1982). The recent finding that the Mesozoic scanilepiform "palaeoniscoids" are the sister taxon to *Polypteridae* indicates that "palaeoniscoids" are an artificial mixture of stem clades and early members of crown clades (Giles et al., 2017). Therefore, unraveling the phylogenetic relationships of these "palaeoniscoids" is critical to reconstructing the early evolutionary history of the clade that comprises one out of every two species of vertebrate on Earth (Near & Thacker, 2024). However, the landmark study of Giles et al. (2017) showed low phylogenetic stability for Mississippian-Early Triassic ray-finned fishes, indicating that further effort is needed to stabilize the relationships of this critical part of the actinopterygian tree.

Objectives

We describe a new species of ray-finned fish, *Tenupiscis dakotaensis* gen. et sp. nov., from the Lower Permian Minnekahta Limestone of South Dakota, USA. The Minnekahta Limestone preserves an abundant but understudied marine assemblage of Permian ray-finned fishes, offering a critical opportunity to help address the paucity of well-preserved fossils of ray-finned fishes from Permian marine deposits and improve our knowledge of the phylogenetic relationships of late Paleozoic and early Mesozoic ray-finned fishes (Friedman, 2015; Friedman & Sallan, 2012; Sallan, 2014). We document the anatomy of *Tenupiscis* from two partially articulated specimens (Field Museum of Natural History FMNH PF 3712 and FMNH PF 3714) and incorporate the new species into parsimony and Bayesian analyses of actinopterygian relationships to infer the phylogenetic position of the new species. Parsimony and Bayesian searches have been unable to resolve the phylogenetic position of new or redescribed Permian actinopterygians relative to late Paleozoic and early Mesozoic taxa (Figueroa et al., 2019; Stack & Gottfried, 2022). The low resolution in these consensus trees could arise from summarizing a broad tree space where topologies have an extremely high amount of variation from widespread uncertainty in the phylogenetic relationships of late Paleozoic and early Mesozoic actinopterygians. Alternatively, the low consensus resolution may arise from a handful of late Paleozoic and early Mesozoic taxa with highly uncertain relationships (i.e., rogues), causing the underlying tree set to be concentrated into islands or clusters of very similar topologies (Maddison, 1991). We calculate and visualize the variation between the trees sampled in each phylogenetic search (i.e., the tree space) to determine if the sampled trees are divided into clusters and search for taxa with deeply conflicting positions in the most parsimonious trees or the Bayesian posterior sample (Smith, 2020a, 2022). The results of our phylogenetic analyses corrected for clustering and rogue taxa illuminate critical patterns in the evolution of ray-finned fishes and the practical applications of tree space to alleviate rogue taxon problems in phylogenetic systematics with morphological data.

Methods

Repositories and institutional abbreviations

CM, Carnegie Museum of Natural History, Pittsburgh, PA, USA; FMNH PF: Field Museum of Natural History, Chicago, Illinois, USA; MSU: Michigan State University, East Lansing, Michigan, USA; NHM, NHMUK: Natural History Museum of the United Kingdom, London, United Kingdom.

Specimen visualization

FMNH PF 3712 and FMNH PF 3714 were photographed with an Olympus E-M5 Mark 2 digital camera with a M. Zuiko Digital ED 14-150MM F4.0-5.6 II lens and a M. Zuiko ED 60mm F2.8 macro lens at the MSU Museum. The built-in image stacking function of the Olympus E-M5 Mark 2 and Helicon Focus (Heliconsoft.com) were used to compile image stacks of FMNH PF 3712. Interpretative drawings were made by tracing digital photographs in Adobe Photoshop while examining each feature under a binocular microscope (Amscope SKU:SM-4NTP) at the MSU Museum. These initial drawings were traced in ink and scanned to make the final panel figures. In our interpretative drawings, dotted lines indicate inferred boundaries, light grey infill indicates space where bone is absent, and dark grey infill indicates space where bone is present but not reliably identifiable.

Terminology

We follow the terminology for early actinopterygian skeletal morphology from Gardiner (1984) to facilitate comparison to historical descriptions. In our descriptions, length refers to the anterior-posterior dimension of the body, depth or height refers to the dorsoventral dimension of the body, and width refers to the mediolateral dimension of the body. Finally, we use the phylogenetic classification of Near & Thacker (2024) to refer to the clade names of ray-finned fishes and adopt PhyloCode where possible (Cantino & de Queiroz, 2010).

Character matrix

We coded the new taxon for 222 discrete morphological characters using the matrix of Stack & Gottfried (2022), which incorporates coding changes from Argyriou et al. (2018) and Coates & Tietjen (2019), adds the early Permian actinopterygian *Concentrilepis minnekahtaensis*, and re-

duces the taxon list to focus on actinopterygian interrelationships (Stack & Gottfried, 2022). The full list of changes is available in the supplementary material of Stack & Gottfried (2022). The full matrix used in our initial analyses contains 10341 scorings for 75 taxa.

We use silhouettes in our phylogenetic tree diagrams to help communicate the taxa associated with different actinopterygian clades. The sources for these silhouettes are as follows, and were created by JS unless otherwise noted: *Acipenser brevirostrum* (Le Sueur, 1818; Phylopic.com, Yan Wong); *Amia calva* (Linnaeus, 1766; Phylopic.com, T. Michael Keesey); *Boreosomus piveteaui* (Nielsen, 1942; modified from Nielsen, 1942, fig. 78); *Cheirolepis canadensis* (Whiteaves, 1881; Phylopic.com, Steven Coombs); *Concentrilepis minnekahtaensis* (modified from Stack & Gottfried, 2022, fig. 23); *Dapedium pholidotum* (Agassiz, 1832; modified from Szabó & Pálfy, 2020, fig. 7); *Hiodon alosoides* (Rafinesque, 1819; Phylopic.com, T. Michael Keesey); *Fouldenia ischiptera* (Traquair, 1881; modified from Sallan & Coates, 2013, fig. 13D); *Luganoia lepidosteoides* (Bürgin, 1992; modified from Xu, 2020 fig.5b and Bürgin, 1992), *Melanecta anneae* (Coates, 1998; modified from Coates, 1998 fig. 1); *Mimipiscus toombsi* (Gardiner & Bartram, 1977; modified from Choo, 2011, fig. 19B); *Polypterus bichir* (Lacépède, 1803; Phylopic.com, T. Michael Keesey); *Platysomus superbus* (Traquair, 1881; modified from Moy-Thomas & Bradley Dyne, 1938, fig. 39).

Parsimony phylogenetic analysis

We integrated the new taxon into a parsimony analysis in TNT 1.5 (Goloboff et al., 2008; Goloboff & Catalano, 2016) and implemented an initial New Technology Search with a combination of the Sectorial Search, Ratchet, Tree Fusing, and Drift algorithms to find the optimal tree length 500 times (random seed =1; Goloboff et al., 2008). We conducted a subsequent traditional search with Tree Bisection and Reconnection on the topologies returned from the New Technology Search. Our strict consensus tree summarizes the agreement between the most parsimonious trees from the traditional search (Nixon & Carpenter, 1996). We also calculated Bremer support values in TNT by conducting Tree Bisection and Reconnection on the most parsimonious trees and allowing the analysis to retain all trees 1-6 steps longer than the optimal length. We calculated the consistency index (CI; Kluge & Farris, 1969) and retention index (RI; Farris, 1989) of the strict consensus in TNT with the stats.run command. We also mapped unambiguous synapomorphies from the most parsimonious trees unto the strict consensus for each analysis in TNT. The use of equal weights parsimony stems from our desire to determine how the addition of *Tenupiscis* altered the results relative to other studies using an altered version of the Giles et al. (2017) framework, primarily Stack & Gottfried (2022). We used PAUP* (Swofford, 2003) to export the strict consensus in a format (.tre) readable by Figtree v1.4.4 (Rambaut, 2018), which we used to make PDF versions to annotate in Adobe Illustrator. Clade names used to annotate our trees are derived from Moore & Near (2020) and Near & Thacker (2024).

Bayesian phylogenetic analysis

We conducted Bayesian phylogenetic inference in MrBayes 3.7.2a using two independent Metropolis-coupled Markov chain Monte Carlo analyses with the MkV model for discrete morphological data (Lewis, 2001; Ronquist et al., 2012). The use of the MkV model stems from our desire to determine how the addition of *Tenupiscis* altered the results relative to other studies using an altered version of the Giles et al. (2017) framework, primarily Stack & Gottfried (2022). Each Metropolis-coupled Markov chain Monte Carlo analysis had four independent Markov chains that ran for an initial 500,000 iterations, with burn-in set to 25% and sampling every 100 generations. We ran 4.5 million generations prior to reaching a standard deviation of split frequencies of 0.008282, with the minimum effective sample size (ESS; Ripley, 1987) exceeding 6000 and the Potential Scale Reduction Factor (PSRF; Gelman & Rubin, 1992) values equal to 1.0. We also used the "plot" command in MrBayes to examine the trend in sampled log-likelihood values to ensure that they are randomly distributed within the space between generations 1,125,000 and 4,500,000, indicating that the chains converged on a stable region of the posterior distribution. Finally, we loaded the probability trace output files from both runs into Tracer 1.7 (Rambaut et al., 2018) and used the Estimates, Marginal Density, and Trace menus to evaluate if the two runs reached the same area of the posterior distribution.

We generated a majority rule consensus tree in MrBayes with the "sumt Burninfrac=0.5" command. We imported the nexus formatted consensus tree into R (R Core Team, 2021) to generate a more flexible annotated consensus tree with the ape (Paradis & Schliep, 2019), phytools (Revell, 2012), and phylotate (Beer & Beer, 2019) packages. The full script for the phylogenetic analysis, the R annotation process (provided by Brenen Wynd, Southeastern Louisiana University), and the consensus file from MrBayes, are available in the Supplementary Data (Dryad link provided post initial submission).

Tree space visualization

We anticipated highly unresolved consensus topologies because previous studies with versions of the matrix of Giles et al. (2017) did not confidently resolve the interrelationships of Mississippian–Triassic "palaeoniscoids" (e.g., Argyriou et al., 2022; Figueroa et al., 2019; Stack & Gottfried, 2022). Low resolution in these consensus topologies could arise from summarizing extremely concentrated clusters of trees (Maddison, 1991) or from a broad tree space where topologies have an extremely high amount of variation. We applied a series of "tree space" techniques for visualizing variation in phylogenetic searches (Smith, 2022; Wright & Lloyd, 2020) to examine the variation in our tree searches. We conducted three parallel studies of tree space in R (R Core Team, 2021), with the cluster (Maechler et al., 2022), TreeTools (Smith, 2019), TreeDist (Smith, 2020b), vioplot (Adler & Kelly, 2022), ape (Paradis & Schliep, 2019), and protoclust (Bien & Tibshirani, 2022) packages. Our analyses are inspired by vignettes by Martin R. Smith

(https://github.com/ms609/TreeDist/blob/HEAD/vignettes/treespace.Rmd; https://ms609.github.io/TreeDist/dev/articles/compare-treesets.html). We examined the most parsimonious trees and 1000 sampled Bayesian trees on their own in addition to a separate analysis of the Bayesian and most parsimonious trees together. A full script and the files needed to recreate these analyses in R is provided in the Supplementary Data.

We calculated the distance between trees via the clustering information distance metric, which Smith (2020a) demonstrated to be the most consistent measure of tree dissimilarity among available metrics. See Smith (2020a) for detailed comparisons and rigorous testing of measures of tree distance. We performed a principal coordinates analysis of each tree sample to create a twelve-dimensional mapping of the distances between the topologies. We calculated the product of the trustworthiness and continuity (TxC; Kaski et al., 2003; Venna & Kaski, 2001) of mappings in 1-12 dimensions to determine how many dimensions were needed to faithfully visually represent the distances between the topologies in each tree sample. The trustworthiness measures the degree to which proximities in the original distance matrix are preserved (Kaski et al., 2003), whereas continuity measures to what degree points that are nearby in the original matrix maintain proximity in the mapping (Smith, 2022; Venna & Kaski, 2001). We mapped each tree space with the number of dimensions needed to meet or surpass a TxC of 0.9, following the recommendation of Smith (2022). We searched for clustering in each tree distance matrix via Partitioning Around Medoids (PAM; Kaufman & Rousseeuw, 1990; with algorithmic improvements from Schubert & Rousseeuw, 2021) and hierarchical clustering with minimax linkage (Hierarchical; Ao et al., 2005; Bien & Tibshirani, 2011) algorithms. We calculated the silhouette coefficient (Kaufman & Rousseeuw, 1990) to evaluate the reliability of the 2-12 clustering structures identified by each algorithm. The silhouette coefficient is a dimensionless measure of the degree to which objects in a cluster are close to other objects in their cluster relative to objects in the closest neighboring cluster (Kaufman & Rousseeuw, 1990).

We further evaluated potential clustering by calculating and visualizing the dispersal of each tree sample, which is the distance between each tree and the respective median tree, to further study the geometry of their respective tree spaces (Smith, 2022). The median tree has the shortest average distance from each other tree in the set (Smith, 2022). Examining the spread of the tree samples about their median allowed us to verify the landscapes shown in the initial tree space analyses. We visualized dispersal between and within the most parsimonious trees and Bayesian tree sample using violin plots (Adler & Kelly, 2022) and density plots, based on a vignette by Tom Kelly, https://cran.r-project.org/web/packages/vioplot/vignettes/violin_area.html).

Rogue taxon search

The landmark study of Giles et al. (2017) showed that Carboniferous and Permian taxa were the least stable in a phylogenetic analysis of actinopterygians with an analysis of leaf stability with RogueNaRok (Aberer et al., 2013). We aimed to determine if any of these unstable taxa acted as rogues in our analysis by conducting a rogue taxon search with the R (R Core Team, 2021) package Rogue (Smith, 2021) on the most parsimonious trees and a sample of 1000 trees randomly sampled from the first run of the Bayesian analysis (accounting for a burn-in of 50%) with the QuickRogue function. We chose to use the Quickrogue function because it can identify rogues as reliably as alternative heuristics in Rogue and RogueNaRok (Aberer et al., 2013) with the benefit of lower computation time (Smith, 2021). Full scripts and datafiles needed to re-run these analyses, which are based on a vignette by Martin R. Smith (https://cran.rproject.org/web/packages/Rogue/vignettes/Bayesian.html), are provided in the Supplementary Data. The Rogue output shows the splitwise phylogenetic information content (the sum of the information content contained in the bipartitions of a topology; Smith, 2021) of the baseline majority rule consensus of the tree sample and the rawImprovement, which shows the change in phylogenetic information content for the removal of each rogue taxon. We compared the rawImprovement scores of each rogue to determine how much information removal they caused relative to each other. The most damaging rogue taxon, "*Kalops monophyrum*", is not one of the two described species of *Kalops* (Poplin & Lund, 2002) and is therefore a *nomen nudum*. Given the rogue behavior of this taxon, we opted to remove "*Kalops monophyrum*" and rescore *Kalops* based on personal examination of the type specimen of *Kalops monophrys* (Poplin & Lund, 2002; CM 27372) and the original description (Poplin & Lund, 2002). The rationale for each character coding change is provided in Part C of the Supplementary Information). We conducted an additional parsimony analysis with "*Kalops monophyrum*" pruned from the matrix, along with a parsimony analysis and Bayesian search with *Kalops monophrys* subbed in for "*Kalops monophyrum*". These searches used identical phylogenetic search and tree space methods to the initial analyses. Revised matrices for each analysis, along with the trees produced by our phylogenetic searches, are provided in the Supplementary Data.

Results

Systematic paleontology

Pan-Actinopterygii Rowe (2004)
[Moore & Near, 2020]
Tenupiscis dakotaensis, gen. et. sp. nov.
urn:lsid:zoobank.org:pub:B2CC9267-19F6-4593-8173-7ECF5F2FE1AF

Derivation of name

Tenu from the Latin Tenuis, meaning fine or thin and piscis from the Latin piscis, meaning fish. Dakotaensis meaning of Dakota, referencing its original collection from South Dakota.

Diagnosis

Dermal cranial bones ornamented with elongate ganoine ridges; two supraorbital elements making up the dorsal portion of the orbit and separating the nasal from the dermosphenotic; separate supratemporal and intertemporal ossifications; three suborbitals (anterior to preopercle, posterior and ventral to dermosphenotic); postorbital plate of maxilla rectangular dorsally and rounded ventrally; subopercle longer than opercle; seven pairs of branchiostegal rays; dorsal most branchiostegal ray longer and taller than the preceding ray; external lateral squamation taller than wide and almost entirely lacking ornament; fringing fulcra absent on the pectoral fin; triangular pectoral fin with a narrow base relative to the width of the fin; triangular dorsal fin set anterior to rounded anal fin; all lepidotrichia lacking ornamentation.

Comparison to existing taxa

Tenupiscis is distinguished from *Concentrilepis* by the cranial ornament of thin ridges on the dentary, maxilla, jugal, median gular, and supracleithrum, the large length of the subopercle relative to the opercle, the presence of seven pairs of branchiostegal rays, the lack of a concentric pattern of ornament on the lateral squamation, and the long and narrow pectoral fin lacking fringing fulcra (Stack & Gottfried, 2022). Although *Concentrilepis* is the only other described actinopterygian from the Minnekahta Limestone, we distinguish *Tenupiscis* from other small (<12 cm in standard length) Mississippian-Permian actinopterygians. *Tenupiscis* differs from the Rhadinichthyidae in having two supraorbital bones between the dermosphenotic and nasal, an enlarged dorsal most branchiostegal ray, and lepidotrichia that are not deeply branched (Lund & Poplin, 1997). Within the Rhadinichthyidae, *Tenupiscis* is distinguished from *Rhadinichthys canobiensis* (Traquair, 1911) in possessing two supraorbitals between the dermosphenotic and nasal, a separate intertemporal and supratemporal, an enlarged dorsal most branchiostegal ray, and the absence of fringing fulcra on the pectoral fin (Moy-Thomas & Bradley Dyne, 1938). *Tenupiscis* can be distinguished from *Palaeoniscum freiselebeni* (de Blainville, 1818; see Part A of the Supplementary Information) by the large size of the subopercle relative to the opercle, the ornamentation of the subopercle and opercle with thin ridges, and the presence of seven pairs of branchiostegal rays (Aldinger, 1937). *Tenupiscis* is differentiated from *Kalops monophrys* (CM 27372) in possessing two supraorbital bones between the dermosphenotic and nasal, a separate intertemporal and supratemporal, the large size of the subopercle relative to the opercle, seven pairs of branchiostegal rays, and the smooth posterior margins of its lateral squamation (Poplin & Lund, 2002). *Tenupiscis* is distinct from *Meisenheimichthys* (NHMUK PV P 76738a/b, NHMUK PV P 76739a/b) in the absence of fringing fulcra on its pectoral fin and the posterior position of its dorsal fin.

Holotype

FMNH PF 3712; articulated, laterally compressed specimen of an actinopterygian preserving the skull, pectoral, pelvic, median, and caudal fins, and most of the lateral squamation (Fig. 1).

Paratype

FMNH PF 3714, posterior cranial elements, partially articulated anterior portion of the trunk, and pectoral fin from a small, elongate actinopterygian. Assigned to *Tenupiscis* based on the lateral squamation being taller than wide and almost entirely lacking ornament.

Occurrence and geologic setting

FMNH PF 3712 and FMNH PF 3714 were collected by Rainer Zangerl, John Clark, and Kenneth Kietzke in a 1962 Field Museum expedition (William Simpson, pers. comm. March 2022) from the Minnekahta Limestone, in the Black Hills region of Rapid City, Pennington County, South Dakota, USA (Fig. 2). The Minnekahta Limestone has a documented fauna of ray-finned fishes, stromatolites, ostracods, gastropods, and pelecypods (Braddock, 1963; Dierks & Pagnac, 2010; Dopheide & Winniger, 2008; Hussakof, 1916).

These strata are interpreted as a transgression of the Phosphoria Seaway, contemporaneous with the Minnekahta Member of the Goose Egg Formation (Wyoming) and the Meade Peak Phosphatic Shale Member of the Phosphoria Formation (S.E. Idaho, western and central Wyoming; Boyd & Maughan, 1972; Burk & Thomas, 1956; Inden & Coalson, 1996; Maughan, 1994; Piper & Link, 2002; Whalen, 1996; Fig. 2E). The conodont biostratigraphy of Behnken (1975) and Wardlaw and Collinson (1986) indicates that the Minnekahta Limestone is late Early Permian in age (Leonardian regional stage, Kungurian global stage, 283.5 +/- 0.6 to 272.95 +/- 0.11 Ma; Cohen et al., 2013; Gradstein et al., 2012).

Description

Skull roof

A laterally compressed ring of bone is preserved from the skull roof in FMNH PF 3712, extending from the tip of the dentary to the posterior edge of the skull. Anteriorly, the intertemporal is a long, roughly triangular element with a narrow, pointed anterior half and a broader posterior half dorsal to the dermosphenotic (Fig. 3). The intertemporal has an anterior contact with the posterior supraorbital and a posterior contact with a broad, oval-shaped supratemporal. A distinct intertemporal and supratemporal is shared with the majority of “palaeoniscoids”, whereas these elements are fused into a paired dermopterotic in a handful of more derived “palaeoniscoids” (i.e., *Guildayichthys carnegiei*; Lund, 2000; J.S. pers. obs. of CM 41071) and crown actinopterygians (Gardiner & Schaeffer, 1989; Grande, 2010; Hilton et al., 2011). A long, thin splinter of

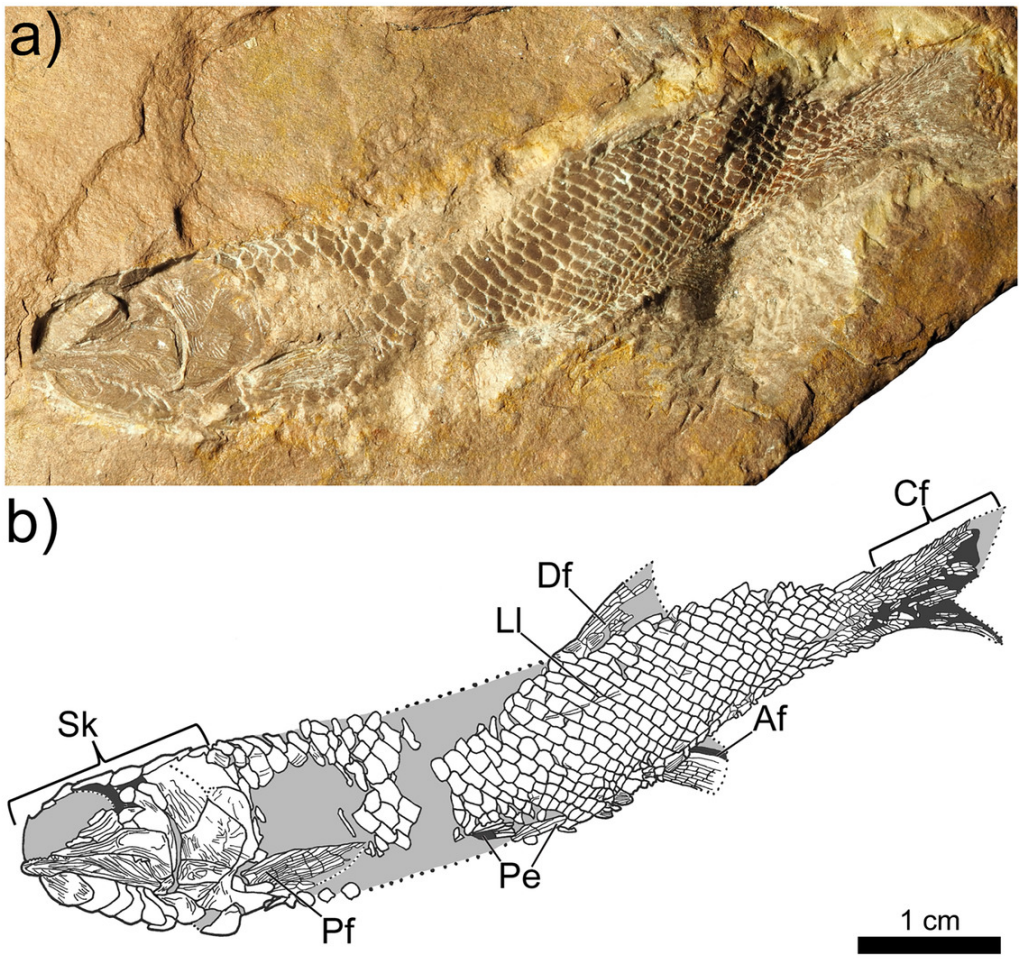

Figure 1. *Tenupiscis dakotaensis* gen. et. sp. nov., holotype specimen (FMNH PF 3712) in left lateral view.

A) photograph. B) line drawing. Scale bar equals 1 cm. Abbreviations: **Af**, anal fin; **Cf**, caudal fin; **Df**, dorsal fin; **Ll**, lateral line; **Pe**, pelvic fin; **Pf**, pectoral fin; **Sk**, skull.

bone (that we cannot identify) is posterior to the supratemporal.

Circumorbital bones

A posteriorly arched nasal extends posteriorly around the dorsal portion of the skull, forming the lateral portion of the snout and anterodorsal edge of the orbit (Fig. 3). Two supraorbitals are visible between the dermosphenotic and the posterior margin of the nasal (Fig. 3). The anterior supraorbital is small and rectangular, whereas the posterior supraorbital is larger, roughly triangular, and broadens posteriorly where it is contacted by the intertemporal and the dermosphenotic. The majority of "palaeoniscoids" do not possess supraorbitals, but are present in the Mississippian *K. monophrys* and *Kalops diophrys* (Poplin & Lund, 2002), which each possessing a ring of supraorbital elements on the dorsal rim of the orbit (Poplin & Lund, 2002). Supraorbitals are also present in the "palaeoniscoids" *Tarrasius*, *Paratarrasius*, *Lambeia*, and *Palaeoniscum* (Aldinger, 1937; Lund & Poplin, 2002; Mickle, 2017). Supraorbitals are a more common feature of early-branching neopterygians and *Acipenser* but are absent in most extant teleosts and *Polypterus* (Gardiner & Schaeffer, 1989; Grande, 2010; Hilton et al., 2011). An impression of a crescent-shaped dermosphenotic is preserved posterior to the supraorbitals in FMNH PF 3712 (Figure 3). The dermosphenotic is contacted ventrally by a broad, crescent-shaped jugal that is laterally ornamented with four posteriorly curved ridges. The jugal is contacted anteriorly by the narrow, unornamented posterior portion of the lacrimal. The anterior portion of the lacrimal is not preserved.

Jaws and dentition

The jaws and associated bones are well-preserved in FMNH PF 3712 (Fig. 3), with only the anterior most section of the upper jaw not preserved. Anteriorly, the maxilla has a long, thin infraorbital projection with a smooth, concave dorsal margin and a convex ventral margin. The maxilla has a broad and expanded postorbital plate, with a flat dorsal margin and a slightly concave posterior margin that both contact the preopercle. The ventral margin expands posteriorly into a large, rounded projection that wraps over the posterior and lateral surface of the lower jaw. A tooth-bearing maxilla with a narrow anterior portion, broad postorbital plate, and firm connection to the preopercle and palatoquadrate is the most common condition observed in "palaeoniscoids" (Gardiner & Schaeffer, 1989). The maxilla is ornamented with long, ventrally curved ridges on its in-

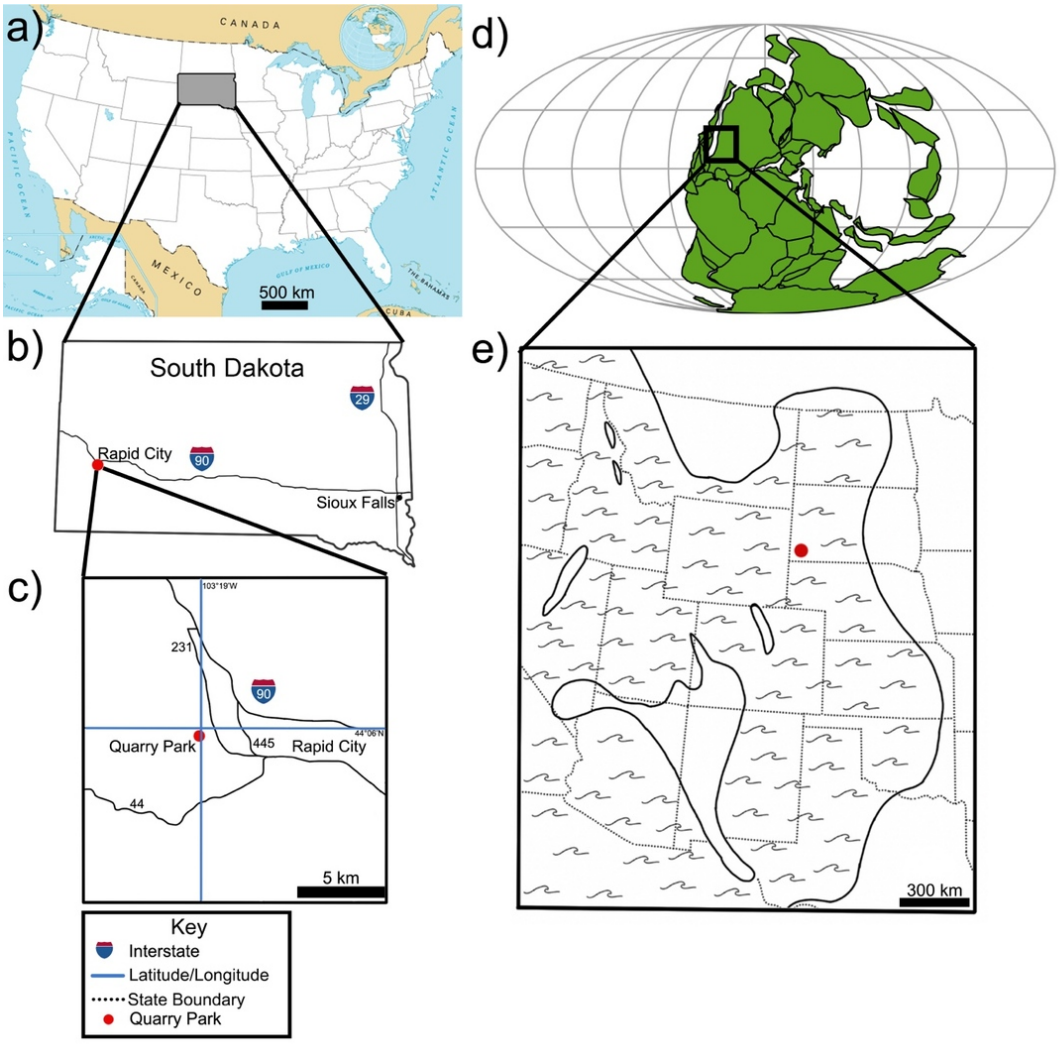

Figure 2. Geographic and paleogeographic context for the Minnekahta Limestone of the Black Hills of South Dakota, USA.

a) South Dakota within the current geography of the continental United States (modified from the National Atlas of the United States). b) Location of Rapid City within South Dakota. c) Location of the Quarry Park locality in Rapid City. d) Location of the western United States within the global paleogeography of the early Permian (Kungurian, ~279 ma). Paleogeographic map generated in the R package chronosphere (Kocsis & Raja, 2020; provided by Davide Foffa (University of Birmingham, UK). e) Location of the quarry park locality within the Permian paleogeography of the western United States (re-drawn from Wilgus & Holser, 1984; figure 1).

fraorbital projection, and thinner ridges on the ventral portion of the postorbital expansion. There are small, pointed, and unornamented teeth on the anterior part of the maxilla and larger teeth lining the ventral margin of the postorbital portion. A long, thin, roughly ellipse-shaped dentary forms the toothed portion of the lower jaw. The dentary has a convex dorsal margin, a concave ventral margin, a narrow, rounded anterior margin, and a broad postorbital section. Small, triangular teeth line the anterior part of the dorsal margin of this bone. The dentary is ornamented with long, thick, and dorsally curving ridges posterodorsally and thinner, straighter, anteroposteriorly oriented ridges anteriorly and ventrally. The left dentary is well-preserved in lateral view in PF 3712, whereas the right dentary is partially visible ventral to the gular and branchiostegal elements. A surangular is partially visible posterior and dorsal to the dentary and ventral to the maxilla, contacting the angular ventrally. This element is mostly obscured by the maxilla. A small, crescentic angular sits directly posterior to the dentary, ventral to the preopercle, ventral and posterior to the surangular, and anterior to the dorsal most branchiostegal rays. The angular is a larger element and more visible in lateral view in "palaeoniscoids" such as *Tenupiscis* and other non-teleosts (Arratia, 2013; Grande, 2010; Grande & Bemis, 1998; Gregory, 1932) than in teleosts. The angular is ornamented with thin, curved ridges.

Opercular series and associated bones

The preopercle is a crescentic element with firm bony connection to the maxilla. The preopercle is thin ventrally and expands as it curves anterodorsally around the posterior margin and over the dorsal margin of the maxilla. This element has a broad, concave, and emarginated anterior edge that contacts the suborbitals anteriorly. The crescent shape and maxillary attachment of the preopercle is typical for a "palaeoniscoid" or a polypterid, whereas derived neopterygians have a narrower, 'C'-shaped preopercle

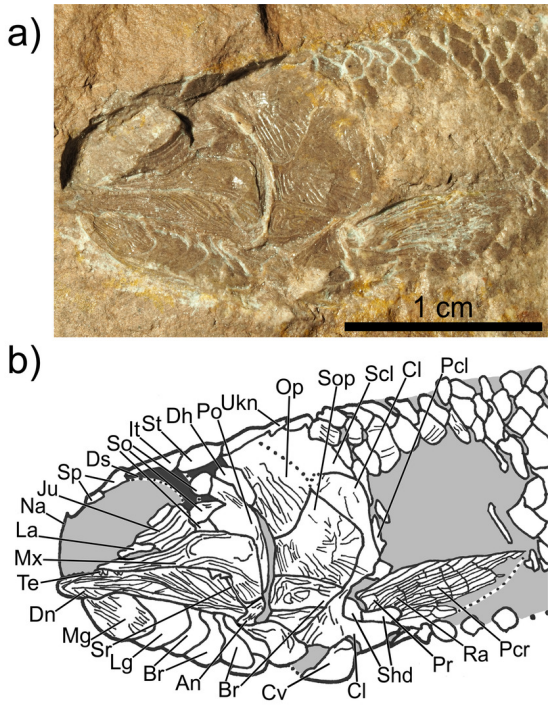

Figure 3. Skull and pectoral fin of *Tenupiscis dakotaensis* gen. et. Sp. nov. in FMNH PF 3712 in left lateral view.

a) photograph. b) specimen drawing. Scale bar equals 1 cm. Abbreviations: **An**, angular; **Br**, branchiostegal ray; **Cl**, cleithrum; **Cv**, clavicle; **Dh**, dermohyal; **Dn**, dentary; **Ds**, dermosphenotic; **It**, intertemporal; **Ju**, jugal; **La**, lacrimal; **Lg**, lateral gular; **Mg,** median gular; **Mx**, maxilla; **Na**, nasal; **Op**, opercle; **Pcl**, post-cleithrum; **Pcr**, pectoral fin rays; **Po**, preopercle; **Pr**, propterygium; **Ra**, radials; **Scl**, supracleithrum; **Shd**, shoulder girdle; **Sop**, subopercle; **Sp**, supraorbital; **St**, supratemporal; **Sr**, surangular; **So**, suborbital; **Te**, teeth; **Ukn**, unknown.

that does not have a bony fusion to the maxilla (Gardiner & Schaeffer, 1989; Grande, 2010; Grande & Bemis, 1998). Thin, dorsoventral ridges ornament the anterior and ventral portion of the preopercle. The dermohyal is a small, unornamented, bean-shaped bone. The dermohyal is nestled directly anterior to the opercle, posterior to the suborbitals, and posterodorsal to the preopercle.

The opercle is a broad element that is posterior to the preopercle and dorsal to the subopercle. The opercle has a complex anterior margin, which is concave anterodorsally about the dermohyal and straight ventrally. The posterior margin of the opercle is broad and convex posteriorly. The dorsal margin of the opercle is straight along a contact with the skull roof, whereas its ventral margin is sinuous as it curves over the subopercle. The expanded ventral portion of this bone is ornamented with long, parallel ganoine ridges, and the narrower dorsal portion lacks ornament. The subopercle is longer than the opercle, sitting directly dorsal to the dorsal most branchiostegal ray and ventral to the opercle. The subopercle is long ventrally and shortens dorsally to a sharp process that fits between the opercle and the supracleithrum. The anterior margin of the subopercle is narrow at the contact with the preopercle, whereas its posterior margin is broad and anteriorly concave where it contacts the supracleithrum and cleithrum. The subopercle is ornamented with short, thin ganoine ridges.

Gulars and Branchiostegals

FMNH PF 3712 preserves a series of branchiostegal rays, along with a corresponding median and lateral gular. The median gular is a large, pointed, roughly oval-shaped bone ornamented with fine, lengthwise ridges. It has a broad, triangular anterior portion and a shorter, rounded posterior portion. The lateral gular is wider and shorter than the median gular. Its anterior margin is concave and wraps around the posterior margin of the median gular. Posteriorly, the lateral gular narrows to a broad point that fits into the concave anterior margin of the first branchiostegal ray. The presence of a median gular and a pair of lateral gulars is the plesiomorphic condition for late Paleozoic "palaeoniscoids", whereas gulars are reduced to one median gular in halecomorphs and elopiform teleosts, reduced in size in polypterids, and are absent in most teleosts and *Acipenseriformes* (Gardiner & Schaeffer, 1989; Grande, 2010; Grande & Bemis, 1991; Hilton et al., 2011; Regan, 1909). The branchiostegal rays extend posteriorly from the lateral gular and wrap around the back of the lower jaw, ending at the base of the subopercle. The size and shape of the brachiostegal rays relative to each other changes considerably from anterior to posterior. The first two branchiostegal rays are sharply curved, with concave anterior margins and convex posterior margins. The third and fourth branchiostegal rays are straighter and thinner than the first two rays. The fifth branchiostegal ray is larger than the preceding elements, with a broad posterior portion contacting the cleithrum. The sixth branchiostegal ray is smaller than the preceding and succeeding rays, with a narrow anterior portion and a broadly pointed posterior portion. The seventh brachiostegal ray is taller than the preceding rays and approximately rhombohedral in shape, with a broad anterior portion that narrows posteriorly. The seventh brachiostegal ray contacts the subopercle dorsally and the cleithrum posteriorly. Although the last three branchiostegal rays are ornamented with concentric, branching ridges, the first three branchiostegal rays lack ornament. We interpret the small element articulated to the fourth and fifth left branchiostegal rays (Fig. 3) as a branchiostegal from the series on the right side of the skull.

Pectoral girdle

The clavicle is a broad, triangular element connected to the ventral part of the cleithrum. A single lateral ridge is the only ornamentation on the clavicle. Paired clavicles are common in late Paleozoic actinopterygians and are present in *Acipenseriformes* and *Polypteridae* but are absent in extant teleosts and the majority of neopterygians (Grande, 2010; Grande & Bemis, 1991). The cleithrum is a tall, curved bone that supports the endoskeletal shoulder girdle and pectoral fin. The broad ventral portion of the cleithrum that curved ventral to the skull *in vivo* is partially flattened laterally. The ventral portion of the cleithrum is broad, roughly triangular, and has a concave posterior margin for the attachment of the pectoral fin. This portion of the cleithrum wraps around the posterior margin of the three dorsal most branchiostegal rays, and is ornamented with long,

sinuous, ganoine ridges. The endoskeletal shoulder girdle connects the pectoral radials to the cleithrum. The tall dorsal portion of the cleithrum broadens as it wraps around the posterior margin of the subopercle and is ornamented with thin ganoine ridges. A thin postcleithrum sits posterior to the cleithrum. The supracleithrum is dorsal to and contacting the cleithrum ventrally and is anteriorly arched along a faint anterior contact with the opercle. The faint contact between the opercle and supracleithrum is most easily observed in the cast of FMNH PF 3712.

Paired fins

The pectoral fin is triangular, with a narrow base and a long leading edge (Fig. 3). The two most proximal pectoral lepidotrichia are each fused along their length, whereas the other pectoral lepidotrichia are thin, closely packed, and segmented throughout. The pectoral lepidotrichia articulate to a series of radials and a single round propterygium at the base of the pectoral fin. Only a small piece of the pelvic fin is preserved in FMNH PF 3712, showing that the pelvic fins are abdominally inserted. The pelvic fin lepidotrichia are thin and regularly segmented (Fig. 1).

Median fins

The dorsal and anal fins are located near the caudal fin on the elongate body of FMNH PF 3712. The preservation of the dorsal fin is faint, showing a triangular fin with its apex in its posterior half (Fig. 4). The dorsal fin lepidotrichia are thin, closely packed, regularly segmented, and distally bifurcating. The segmentation becomes more frequent in the distal portion of the fin. There are two pointed, wedge-shaped dorsal basal fulcra anterior to the dorsal fin. The dorsal basal fulcra have thin, lengthwise ridges that are not present on the body scales near them. The anal fin is small, round, inserts posterior to the dorsal fin, and has thin, regularly segmented lepidotrichia (Fig. 5). The leading edge of the anal fin is not well-enough preserved to determine if it had fringing fulcra. Additionally, the posterior and distal portions of the fin are poorly preserved. Two pairs of anal basal fulcra sit anterior to the anal fin, distinguishable from the surrounding squamation by their rounded shape, larger size, and oblique orientation. These fulcra are ornamented with thin ganoine ridges. Three ventral ridge scales, also rounded and enlarged, are anterior to the anal basal fulcra.

Caudal fin

The dorsal lobe of the caudal fin is well-preserved in FMNH PF 3712, but the medial portion of the fin and the ventral lobe are faint (Fig. 6). The caudal fin is heterocercal, forked, and has a broad dorsal lobe and a shorter, more slender ventral lobe. The dorsal lobe is lined with thin, pointed, wedge-shaped caudal basal fulcra that grade into a series of smaller fringing fulcra posteriorly, extending for the preserved length of the fin. The base of the ventral lobe of the caudal fin is lined with basal fulcra that shorten and narrow posteriorly. We do not observe any fringing fulcra in the ventral lobe of the caudal fin. The lepidotrichia in the dorsal part of the caudal fin are thin, closely packed, and segmented to their bases. The lepidotrichia in the ventral lobe are thin, closely packed, and segmented.

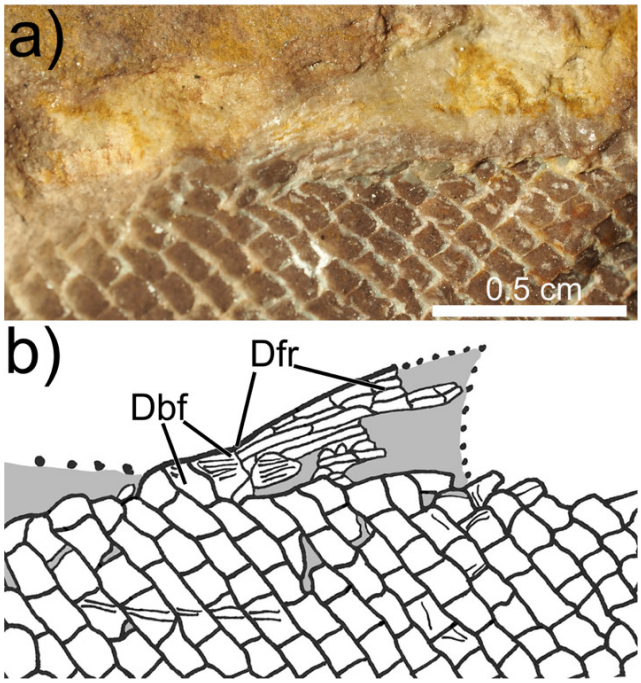

Figure 4. Dorsal fin of *Tenupiscis dakotaensis* in FMNH PF 3712, left lateral view.

a) photograph. b) specimen drawing. Scale bar equals 0.5 cm. Abbreviations: **Dbf**, dorsal basal fulcra; **Dfr**, dorsal fin rays.

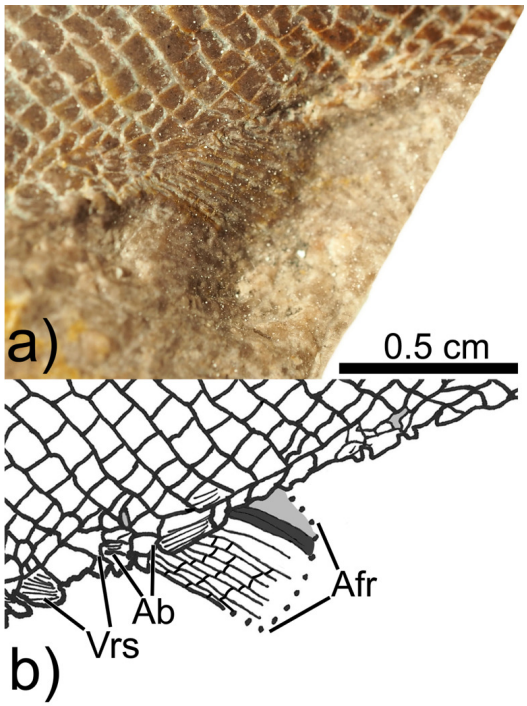

Figure 5. Anal fin of *Tenupiscis dakotaensis* in FMNH PF 3712, in left lateral view.

a) photograph. b) specimen drawing. Scale bar equals 0.5 cm. Abbreviations: **Ab**, anal basal fulcra; **Afr**, anal fin rays; **Vrs**, ventral ridge scales.

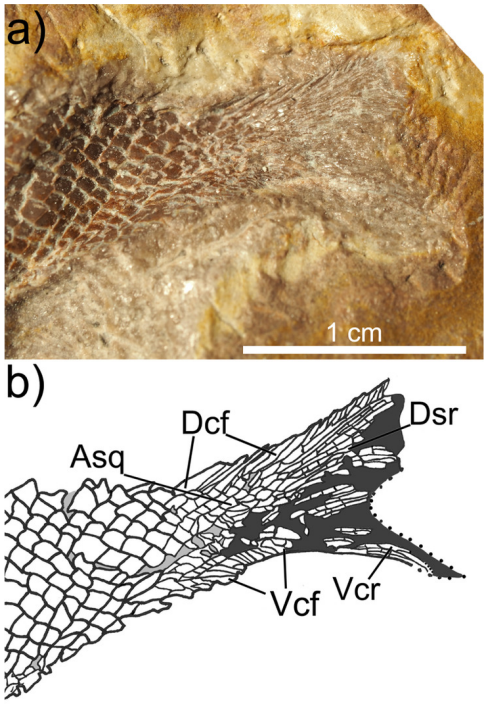

Figure 6. Caudal fin of *Tenupiscis dakotaensis* in FMNH PF 3712, in lateral view.

A, photograph. B, specimen drawing. Scale bar equals 1 cm. Abbreviations: **Asq,** axial squamation; **Dcf**, dorsal caudal lobe basal fulcra; **Dsr**, dorsal caudal fin rays; **Vcf**, ventral caudal lobe basal fulcra; **Vcr**, ventral caudal lobe fin rays.

Squamation

Rhombic, ganoine scales cover the preserved portions of the bodies of FMNH PF 3712 (Fig. 1) and FMNH PF 3714. The scales tend to be more rounded than the typical rhombohedral shape for Paleozoic actinopterygians (Schultze, 2016), and the vast majority lack ornamentation. A few scales on the dorsal nape and the insertion of the dorsal and anal fins bear thin, curved ridges. The scales in the lateral flank region are taller than broad, shortening dorsally and ventrally from the midline. The scales are shorter, more dorsoventrally compressed, and more diamond-shaped in the region between the anal fin and the tail. Additionally, the scales are smaller and more diamond-shaped in the region surrounding the base of the anal fin. A similar pattern is not present surrounding the base of the dorsal fin. A portion of the lateral line is preserved in the midsection of the body between the dorsal and anal fin insertions (Fig. 1). Dorsal ridge scales are present along the preserved portion of the dorsal body margin near the head. The dorsal ridge scales are small and curved anteriorly, with a pointed dorsal margin and a thicker, rounded ventral portion. These grade posteriorly into flatter, shortened, less curved, and thicker scales.

Results of phylogenetic analyses

Initial parsimony phylogenetic search

The parsimony analysis with a heuristic search resulted in 380 most parsimonious trees (MPTs) of length 1088, summarized in a strict consensus (Fig. 7). Beginning at the root of the tree and proceeding towards the tips, Devonian actinopterygians resolve as a grade separate from all other actinopterygians after *Cheirolepis*. A clade containing Carboniferous and Triassic actinopterygians, including *Boreosomus*, *Luederia kempi* (Schaeffer & Dalquest, 1978), *Coccocephalichthys wildi* (=*Cococephalus wildi*; Watson, 1925), *Kansasiella eatoni* (Poplin, 1974), *Trawdenia planti* (Coates & Tietjen, 2019), and *Lawrenciella schaefferi* (Hamel & Poplin, 2008), branches off prior to *Actinopterygii* with low stability (Bremer support = 1). The common synapomorphies for this unnamed clade in the 380 most parsimonious trees are anocleithrum, bone absent (0>2); branchiostegal rays – dorsal-most in series, deeper than adjacent branchiostegal ray (0>1); pronounced median anterior crista on dorsal surface of braincase, present (0>1). *Actinopterygii* is an enormous polytomy (Bremer support = 2), including the neopterygians, *Polypteridae+Scanilepiformes*, pan-acipenseriforms, and sixteen "palaeoniscoids". The common synapomorphies for *Actinopterygii* in the 380 most parsimonious trees are premaxilla as distinct ossification, absent (0>1); premaxilla contributes to oral margin, absent (1>0); tube-like canal bearing arm of the antorbital, absent (1>0); sensory canal/pit line associated with maxilla, present (1>0); teeth of outer dental arcade, single row of teeth (1>2); ventral cranial fissure and vestibular fontanelle, confluent (0>1); hypophyseal chamber, projects posteroventrally (1>0); ventral scutes between hypochordal lobe of caudal and anal fin, absent (1>0). The "palaeoniscoids" within this this polytomy include a mix of Carboniferous, Permian, and Triassic taxa, including *Tenupiscis* and *Concentrilepis*, which are recovered as sister taxa with low stability (Bremer support = 1). The common synapomorphies for the grouping of *Tenupiscis* and *Concentrilepis* are basal scutes on fins, present (0>1) and caudal fin geometry, short chordal lobe (0>1). Eurynotiformes, including *Amphicentrum granulosum* (Young, 1866), *Fouldenia*, and *Styracopterus fulcratus* (Traquair, 1881), form a clade with higher stability (Bremer support = 3) at the base of *Actinopterygii* (Sallan & Coates, 2013). Eurynotiformes have the following common synapomorphies in the most parsimonious trees teeth on premaxillae, absent (0>1); teeth on dentary, absent (0>1); jaw margins overlain by lateral lamina, present (0>1). *Pan-Neopterygii* includes the Late Mississippian (Namurian) *Discoserra pectinodon* (Lund, 2000) and *Bobasatraniidae* (*Bobasatrania groenlandica* Stensiö, 1932; *Ebenaqua ritchiei* Campbell & Phuoc, 1983) with higher stability (Bremer support = 3). The common synapomorphies for pan-neopterygians in the most parsimonious trees are expanded dorsal lamina of maxilla, absent (1>0); number of cheek bones bearing pre-opercular canal posterior to jugal, multiple (0>1); hyoid facet, horizontal (0>1); clavicle, much reduced or absent (0>1).

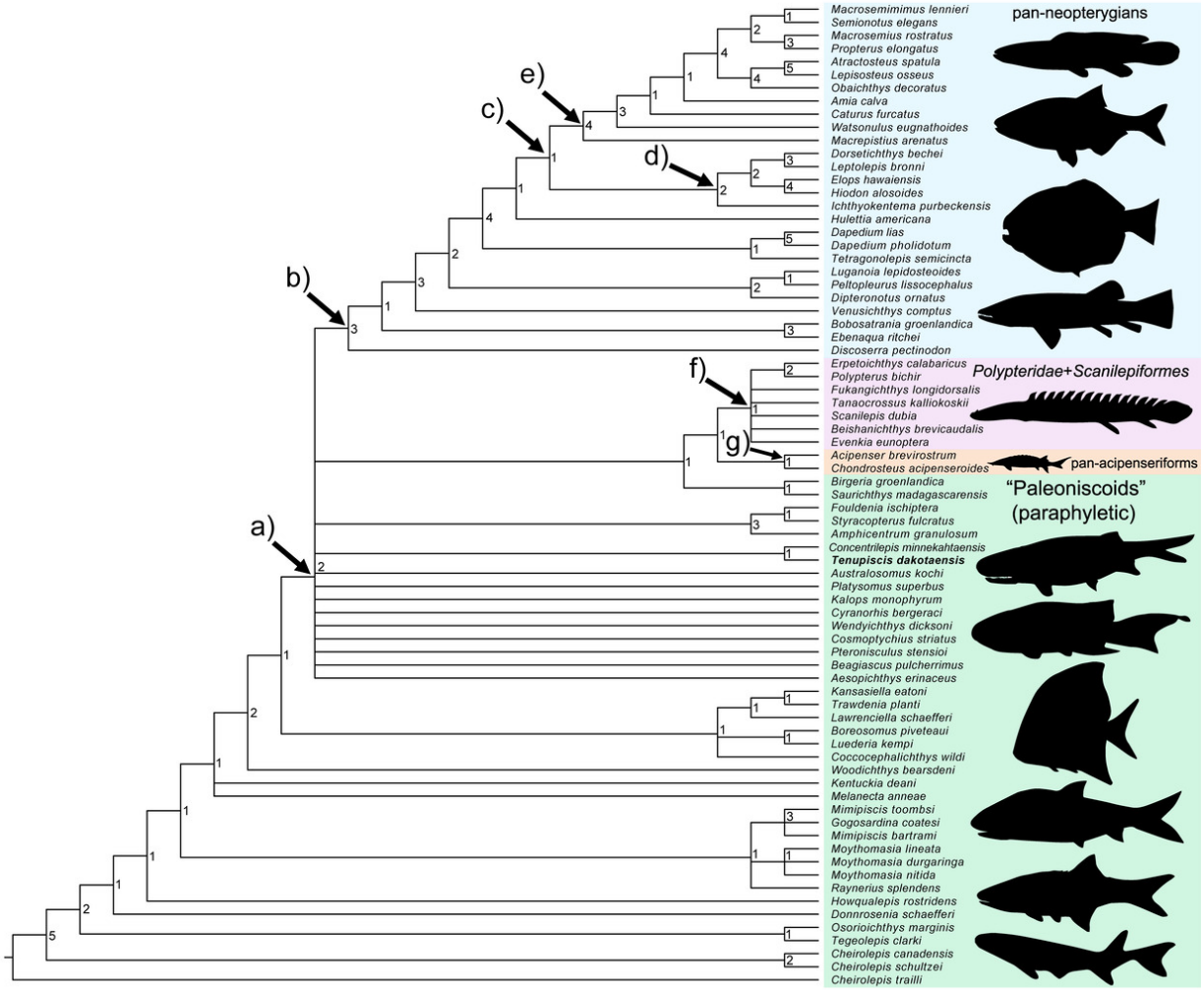

Figure 7. Relationships of *Tenupiscis* from a strict consensus of 380 most parsimonious trees of length 1088 from a parsimony analysis of 75 taxa and 222 morphological characters modified from from Giles et al. (2017).

Nodes annotated with Bremer decay indices. Consistency index = 0.213, retention index = 0.584. Abbreviations: a), *Actinopterygii*. b), pan-neopterygians. c), *Neopterygii*. d), pan-teleosteans. e), pan-holosteans. f), *Polypteridae+Scanilepiformes*. g), pan-acipenseriforms. Silhouettes (in order from top to bottom): *Amia*; *Hiodon*; *Dapedium*; *Luganoia*; *Polypterus*; *Acipenser*; *Concentrilepis*; *Fouldenia*; *Platysomus*; *Boreosomus*; *Mimipiscus*; *Cheirolepis*.

Initial Bayesian phylogenetic search

The majority rule consensus tree from the Bayesian phylogenetic analysis (Fig. 8) shows that *Cheirolepis schultzei* (Arratia & Cloutier, 2004) and *Cheirolepis canadiensis* form a group separate from other Devonian actinopterygians with an estimated posterior probability of 1. The grouping of Devonian actinopterygians outside of *Cheirolepis* also has strong support with an estimated posterior probability value of 1, forming a polytomy. Fifteen species of "palaeoniscoids", including *Tenupiscis*, form a large polytomy with *Actinopterygii* (estimated posterior probability of 0.64). Among the deep-bodied "palaeoniscoid" taxa, there is relatively low support (estimated posterior probability of 0.65) for a clade containing a representative guildayichthyid (*Discoserra*) and two bobasatraniids (*Ebenaqua* and *Bobasatrania*). Conversely, there is strong support (estimated posterior probability of 0.94) for a eurynotiform grouping (*Styracopterus*, *Fouldenia*, and *Amphicentrum*). *Saurichthys madagascariensis* (Piveteau, 1945) and *Birgeria groenlandica* (Stensiö, 1932) are separate from the pan-acipenseriforms (*Acipenser* and *Chondrosteus acipenseroides*; Egerton, 1858) and polypterids in this consensus tree, unlike the initial parsimony strict consensus. There is strong support (estimated posterior probability of 0.95) for a clade containing the *Scanilepiformes* and *Polypteridae*.

Tree space visualization of the initial most parsimonious trees and the Bayesian tree sample

The most parsimonious trees are less dispersed than the Bayesian tree sample (Fig. 9a). The dispersal values of the most parsimonious trees are lower (Fig. 9a) and show a bimodal distribution (Fig. 9b), whereas the dispersal values of the Bayesian tree sample are higher (Fig. 9a) and have an approximately unimodal distribution (Fig. 9c). This dispersal pattern indicates that the most parsimonious trees

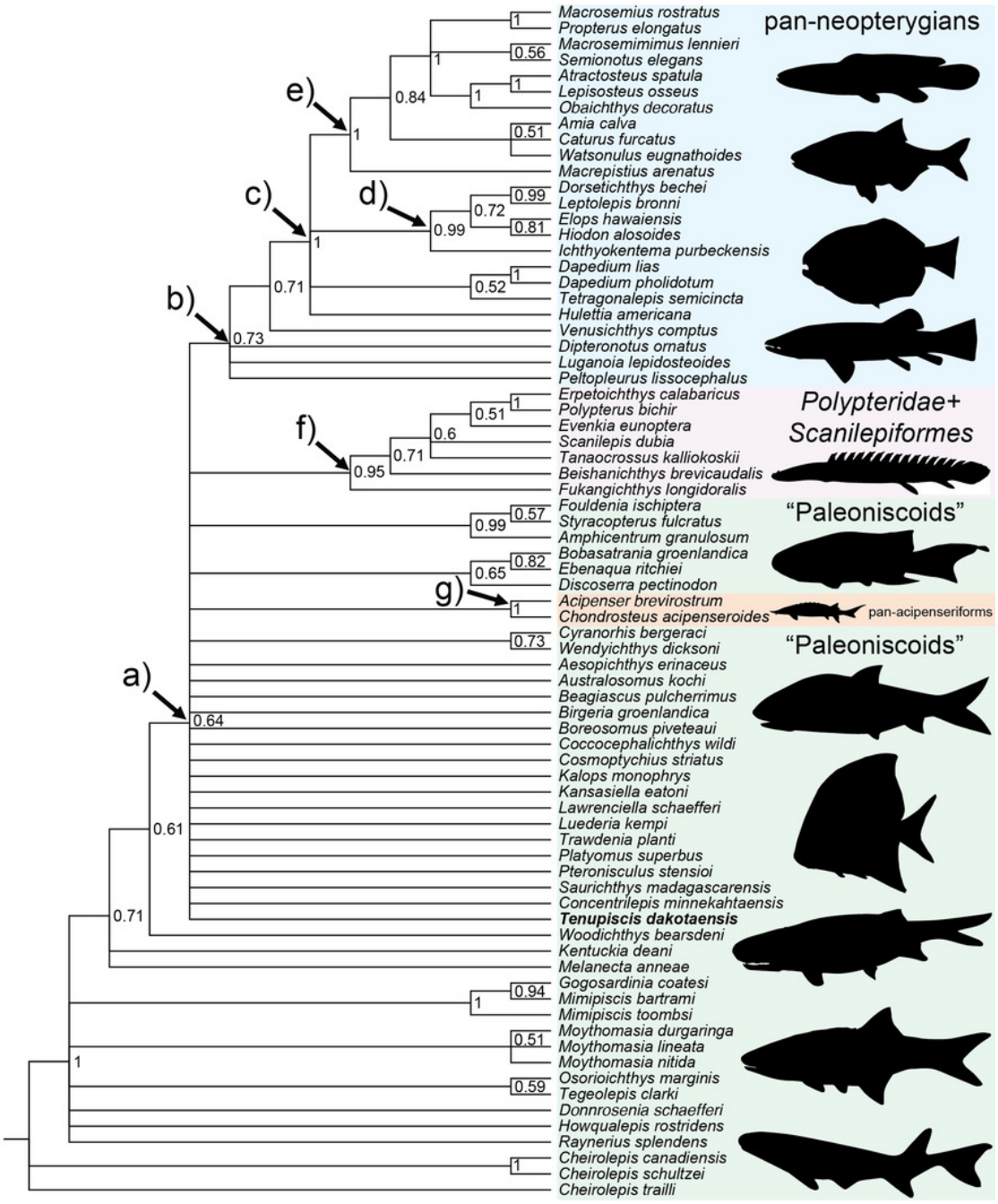

Figure 8. Relationships of *Tenupiscis* from a majority rule consensus tree from a Bayesian analysis of 75 taxa and 222 discrete morphological characters modified from Giles et al. (2017). Phylogenetic hypothesis of actinopterygian interrelationships based on estimated posterior probabilities greater than 0.5 (posterior probability labeled at splits), splits with estimated posterior probability less than 0.5 are condensed to polytomies.

a), *Actinopterygii*. b), pan-neopterygians. c), *Neopterygii*. d), pan-teleosteans. e), pan-holosteans. f), *Polypteridae+Scanilepiformes*. g), pan-acipenseriforms. Silhouettes (in order from top to bottom): *Amia*; *Hiodon*; *Dapedium*; *Luganoia*; *Polypterus*; *Fouldenia*; *Acipenser*; *Boreosomus*; *Platysomus*; *Concentrilepis*; *Mimipiscus*; *Cheirolepis*.

are concentrated about two clusters, whereas the Bayesian trees are more evenly distributed around their median.

We searched for clusters in the most parsimonious and Bayesian trees to investigate the patterns in the dispersal visualizations. Our cluster search estimates the silhouette coefficient of two clusters in the most parsimonious trees as surpassing a "reasonable" threshold of 0.5 (Kaufman & Rousseeuw, 1990) with both partitioning around medoids (PAM; 0.58) and hierarchical clustering with minimax linkage (0.58; Fig. 10a; Bien & Tibshirani, 2011). This indicates that the most parsimonious trees are drawn from two primary clusters with some imperfect overlap. Therefore, they do not match the accepted definition of tree "islands", which stipulates that the subsets be mutually exclusive (Hendy et al., 1988; Silva & Wilkinson, 2021). The highest silhouette coefficient from an identical cluster search for the sampled initial Bayesian trees does not approach the 0.5 threshold for 2 clusters (0.07 for PAM and 0.03 for hi-

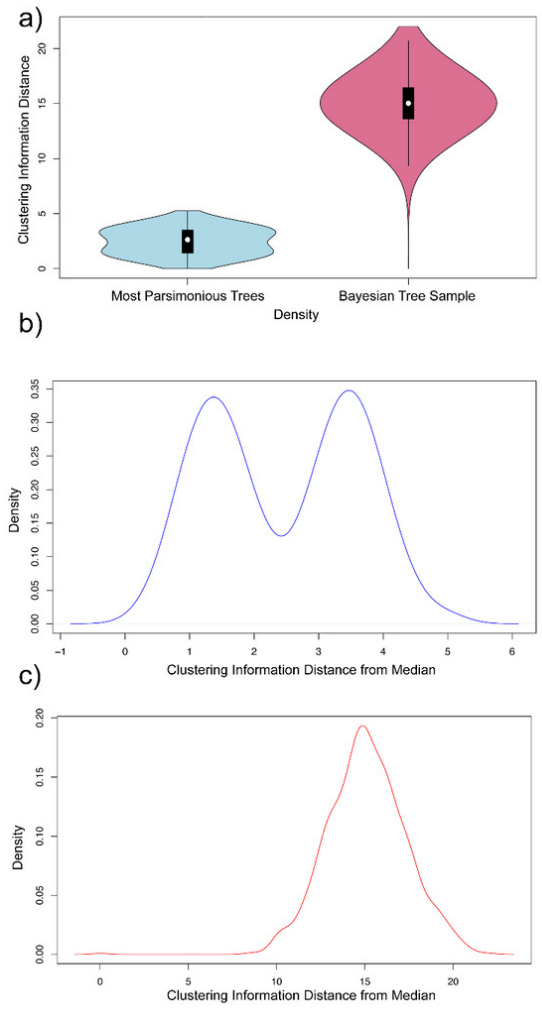

Figure 9. Visualization of the dispersal of the most parsimonious trees and Bayesian tree samples about their respective median.

a) Violin plot comparing dispersal in the most parsimonious trees and Bayesian tree sample. b) Dispersal plot showing the distribution of the distance of the most parsimonious trees from the median most parsimonious tree. c) Dispersal plot showing the distribution of the distance of the sampled Bayesian trees from the median sampled Bayesian tree.

erarchical clustering with minimax linkage; Supplementary Information Part D), strongly suggesting a more widely dispersed (i.e., unclustered) tree space. The topological variation within the two clusters shows identical uncertainty in the interrelationships of some Devonian genera (*Moythomasia durgaringa* Gardiner & Bartram, 1977; *Gogosardinia coatesi* Long et al., 2008; *Mimipiscus*), among the clade *Polypteridae+Scanilepiformes*, and between *Luganoia*, *Peltopleurus lissocephalus* (Brough, 1939), and *Dipteronotus ornatus* (Bürgin, 1992). The strict consensus trees from each cluster of most parsimonious trees differ only in the position of "*Kalops monophyrum*". Therefore, the most parsimonious trees from the initial search are divided into two clusters distinguished by a single terminal taxon.

Rogue taxon search

Our rogue taxon search identified a single rogue from the most parsimonious trees and six rogues from the sample of the Bayesian trees. "*Kalops monophyrum*" was the only rogue taxon found in the most parsimonious trees (Table 1a). The rawImprovement of "*Kalops monophyrum*" was 411.651, meaning that the information content of the consensus tree with it removed improved by more than 25% relative to the original consensus. The rogue taxon search of the Bayesian tree sample found that "*Kalops monophyrum*", along with *Aesopichthys erinaceus* (Poplin & Lund, 2000), *Tenupiscis*, *Peltopleurus*, *Chondrosteus*, and *Acipenser* qualify as rogues (Table 1b). The removal of those taxa, except for *Acipenser*, improved the information content of a majority rule consensus of the Bayesian tree sample. The removal of *Tenupiscis*, *Chondrosteus*, and *Peltopleurus* had the largest information content improvement – over four times the improvement from removing *Kalops* and *Aesopichthys*. The individual rawImprovement scores for each of these rogue taxa does not surpass 12% of the information content of the baseline consensus. Therefore, the lone rogue in the parsimony search caused more information to be lost from the consensus tree than any of the individual rogues in the Bayesian search.

Parsimony search with "Kalops monophyrum" removed from matrix

Our parsimony analysis with "*Kalops monophyrum*" removed from the matrix, i.e., our "restricted search", recovered a better resolved picture of late Paleozoic actinopterygian evolutionary relationships. We see the most topological change amongst the late Paleozoic "palaeoniscoids" in the strict consensus of the most parsimonious trees (Fig. 11). Devonian "palaeoniscoids" still resolve separately from post-Devonian taxa. However, the positions of late Paleozoic "palaeoniscoids" relative to each other and to extant clades are far more resolved in the analysis with the rogue taxon removed. The strict consensus of the initial parsimony search placed 14 Carboniferous–Triassic "palaeoniscoids", including *Tenupiscis*, in a polytomy in the actinopterygian stem group (Fig. 11). In contrast, the strict consensus of the restricted search resolves the Mississippian *Aesopichthys*, *Beagiascus pulcherrimus* (Mickle et al., 2009), *Cyranorhis bergeraci* (Lund & Poplin, 1997), *Wendyichthys dicksoni* (Lund & Poplin, 1997), and *Cosmoptychius striatus* (Watson, 1928), along with *Concentrilepis*, *Tenupiscis* and the Early Triassic *Pteronisculus stensioi* (Nielsen, 1942) as a clade within the actinopterygian stem group (Fig. 11). The common synapomorphies for this clade in the most parsimonious trees are shape of parietals (sarcopterygian postparietals), quadrate (0>1); antorbital bone, present (0>1); suborbitals (non-canal bearing ossifications separating jugal and maxilla), two (0>2); operculum, relative size, at least twice as high as suboperculum (1>0). Our revised strict consensus also places *Tenupiscis* as the sister taxon of *Concentrilepis*, with the same common synapomorphies as the initial parsimony analysis. This "palaeoniscoid" clade resolves separately from *Actinopterygii*, the

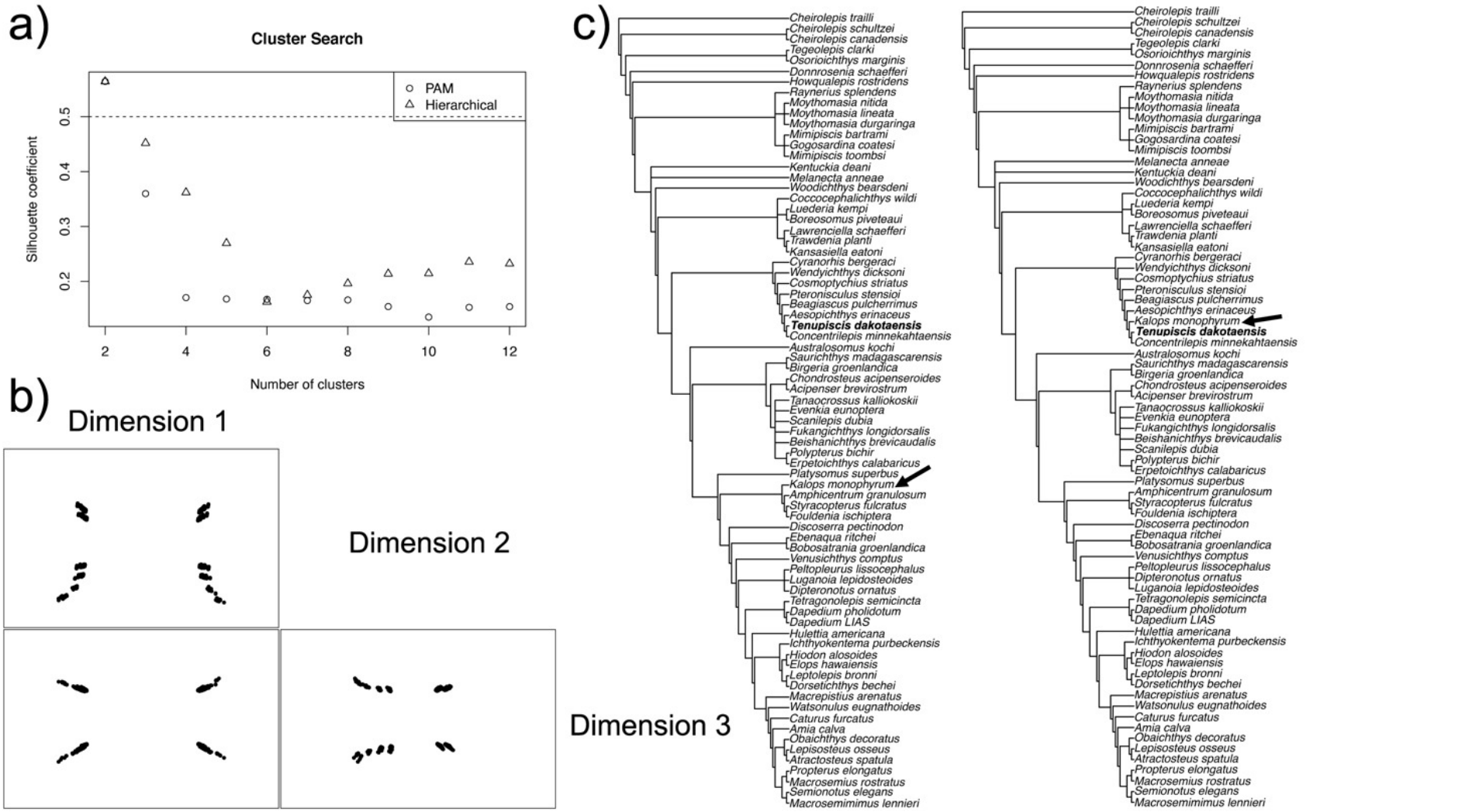

Figure 10. Cluster search for the most parsimonious trees recovered in the parsimony analysis.

a) Silhouette coefficient of trees divided into increasing numbers of clusters identified by partitioning around medoids (PAM; Kaufman & Rousseeuw, 1990) and hierarchical clustering with minimax linkage (Hierarchical; Murtagh, 1983). b) Three-dimensional tree space PcoA visualization of the most parsimonious topologies. c) Strict consensus trees (frequency threshold = 1) of the most parsimonious topologies divided into two clusters. The location of "*Kalops monophyrum*", the only terminal taxon whose position changes between the two topologies, is indicated with arrows.

Table 1. Rogue taxa identified in the most parsimonious trees (a) and 1000 trees from the Bayesian sample of the posterior distribution of trees (b). These tables show how removal of each taxon (taxNum, Taxon) improved the splitwise phylogenetic information content (rawImprovement, IC; Smith, 2021) of the majority rule consensus topology of each tree set.

(a)

taxNum	Taxon	rawImprovement	IC
NA	NA	NA	1437.886
47	*"Kalops monophyrum"*	411.651	1849.537

(b)

taxNum	Taxon	rawImprovement	IC
NA	NA	NA	627.122
2	*Aesopichthys erinaceus*	9.363	636.485
75	*Tenupiscis dakotaensis*	76.229	712.715
57	*Peltopleurus lissocephalus*	43.474	756.189
37	*"Kalops monophyrum"*	10.744	766.933
1	*Acipenser brevirostrum*	-12.195	754.737
16	*Chondrosteus acipenseroides*	58.601	813.338

common synapomorphies for which are foramen for abducens nerve (VI) dorsally positioned (level with optic foramen (II), absent (1>0); dorsal aorta pierced by canal/s for exit of eff.a.2, absent (1>0); parasphenoid teeth, absent (0>2); basihyal, absent (1>0); number of hypobranchials, three (1>0); dorsal scutes anterior to dorsal fin, absent (1>0); ventral scutes anterior to anal fin, absent (1>0); median neural spines in caudal region, present (0>1).

The Mississippian–Pennsylvanian deep-bodied *Platysomus*, *Fouldenia*, *Amphicentrum*, and *Styracopterus* are resolved at the base of the neopterygian stem group in the restricted strict consensus (Fig. 11). Pan-neopterygians, including these deep-bodied taxa, has the following common synapomorphies: premaxilla fused at midline, present (0>1); shape of parietals (sarcopterygian postparietals), quadrate (0>1); dermohyal, absent (1>0); number of infradentaries, one (angular only, 1>2); buccohypophyseal canal pierces parasphenoid, present (1>0). The gain in resolution is not restricted to the interface of the actinopterygian stem and crown. The polytomy of *Dipteronotus*, *Luganoia*, and *Peltopleurus* from the initial search is resolved with *Luganoia* being the sister taxon of *Peltopleurus* in the restricted search. The common synapomorphies for the sister grouping of *Luganoia* and *Peltopleurus* are antorbital bone, absent (1>0); dorsal scutes anterior to dorsal fin, absent (1,2>0).

The tree space of the restricted parsimony search does not show two clusters (Fig. 12). Although visual inspection of the lower dimensions of the restricted search tree space mapping suggests some division between two areas, both of our cluster search algorithms for two clusters yield silhouette coefficients less than 0.5 (0.18 for PAM and 0.39 for hierarchical clustering with minimax linkage), below the "reasonable" threshold of Kaufman and Rousseeuw (1990). The low silhouette coefficients shows that the potential clusters in the tree space mapping overlap with each other more than is visually apparent in a two-dimensional projection, indicating that the data are not divided into two distinct clusters. Further, the dispersal of the restricted most parsimonious tree search has one primary peak, indicating that the tree sample is not strongly concentrated into two clusters. Similarly, a rogue taxon search yielded no rogues in the tree set. The cluster searches and dispersal, when compared to those of the initial parsimony search, indicate that the gain in resolution in the strict consensus is due to summarizing a tree space that is not sharply divided into two clusters.

Parsimony search with "Kalops monophryum" recoded as Kalops monophrys

Recoding *Kalops* (based on the type specimen of *Kalops monophrys*, CM 27372; see Materials and Methods for details) to replace "*Kalops monophryum*" created substantial changes in the strict consensus resolution of "palaeoniscoids" when compared to the strict consensus of the initial parsimony analysis (Fig. 7). The Eurynotiformes (represented here by *Fouldenia*, *Styracopterus*, and *Amphicentrum*) resolve at the base of the neopterygian stem with *Platysomus*. Pan-neopterygians have identical common synapomorphies in this tree to the analysis where *"Kalops monophryum"* was removed. The other taxa that were recovered in a polytomy at the base of *Actinopterygii* in the initial parsimony analysis are resolved as a clade of stem actinopterygians with relatively low stability (Bremer support = 1). The common synapomorphies for this clade identical to those in the analysis where *"Kalops monophryum"* was removed. These include *Tenupiscis* within a polytomy of *Aesopichthys*, *Beagiascus*, and a pairing of *Concentrilepis* and *Kalops*. The grouping of these taxa has one common synapomorphy in the most parsimonious trees, three or more suborbitals (0>2). The sister grouping of *Concentrilepis* and *Kalops* has the common synapomorphies of premaxilla, fused at midline, present (0>1); frontals broad pos-

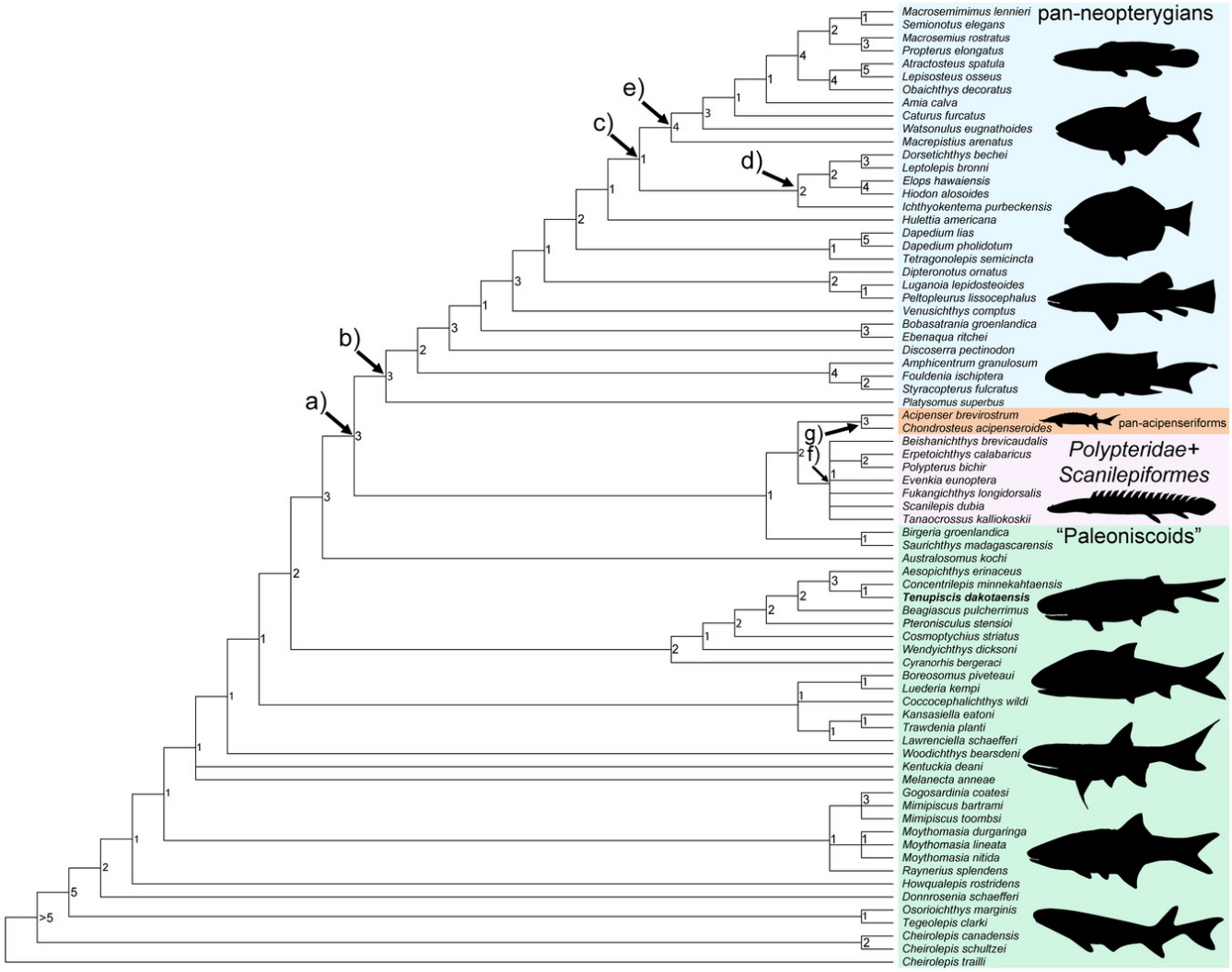

Figure 11. Relationships of *Tenupiscis dakotaensis* gen. et. sp. nov. from a strict consensus of 190 most parsimonious trees of length 1076 from a parsimony analysis of 74 taxa (with the rogue taxon "*Kalops monophyrum*" removed) and 222 morphological characters modified from Giles et al. (2017).

Nodes annotated with Bremer decay indices. Consistency index = 0.231 and retention index = 0.620. Abbreviations: a) *Actinopterygii*; b) pan-neopterygians; c) *Neopterygii*; d) pan-teleosteans; e) pan-holosteans; f) *Polypteridae+Scanilepiformes*; g) pan-acipenseriforms. Silhouettes (in order from top to bottom): *Amia*; *Hiodon*; *Dapedium*; *Luganoia*; *Fouldenia*; *Polypterus*; *Acipenser*; *Concentrilepis*; *Boreosomus*; *Melanecta*; *Mimipiscus*; *Cheirolepis*.

teriorly and tapering anteriorly, present (0>1); infraorbitals, more than two (1>2); small scales below dorsal fin, present (0>1). A second polytomy containing *Cosmoptychius*, *Cyranorhis*, *Pteronisculus*, and *Wendyichthys* is the sister taxon to the grouping containing *Tenupiscis*. Resolution was also lost in other "palaeoniscoids". There is a polytomy containing *Boreosomus*, *Coccocephalichthys*, *Kansasiella*, *Lawrenciella*, *Luederia*, and *Trawdenia* in the strict consensus of the recoded analysis (Fig. 13). The only other change in strict consensus topology between the initial and recoded analyses is that *Luganoia* and *Peltopleurus* are sister taxa in the recoded consensus as in the strict consensus of the analysis where *"Kalops monophryum"* was removed, with *Dipteronotus* as their closest relative; these taxa were in a trident polytomy in the strict consensus of the initial analysis. In all other respects, the initial and recoded analyses have identical strict consensus topologies.

Our recoded *K. monophrys* had a total of 110 missing characters and four inapplicable characters out of 222 total characters, in contrast to the original "*Kalops monophyrum*", which had 98 missing and 12 inapplicable characters. However, the recoded *K. monophrys* is no longer a rogue in our follow-up parsimony search despite having more missing characters. PAM and Hierarchical 2-12 cluster solutions for the recoded analysis all had silhouette coefficients below 0.5, showing little evidence for clustering. Additionally, the dispersal of the recoded most parsimonious tree space is more concentrated into one peak than the initial search. The rogue taxon search on the recoded analysis returned zero rogues, further indicating that *Kalops* no longer acts as a rogue and that the most parsimonious tree space from the recoded analysis is not concentrated in two clusters. *K. monophrys* is the sister taxon to *Concentrilepis* within the clade of stem actinopterygian "palaeoniscoids" (including *Tenupiscis*). This revised placement suggests that

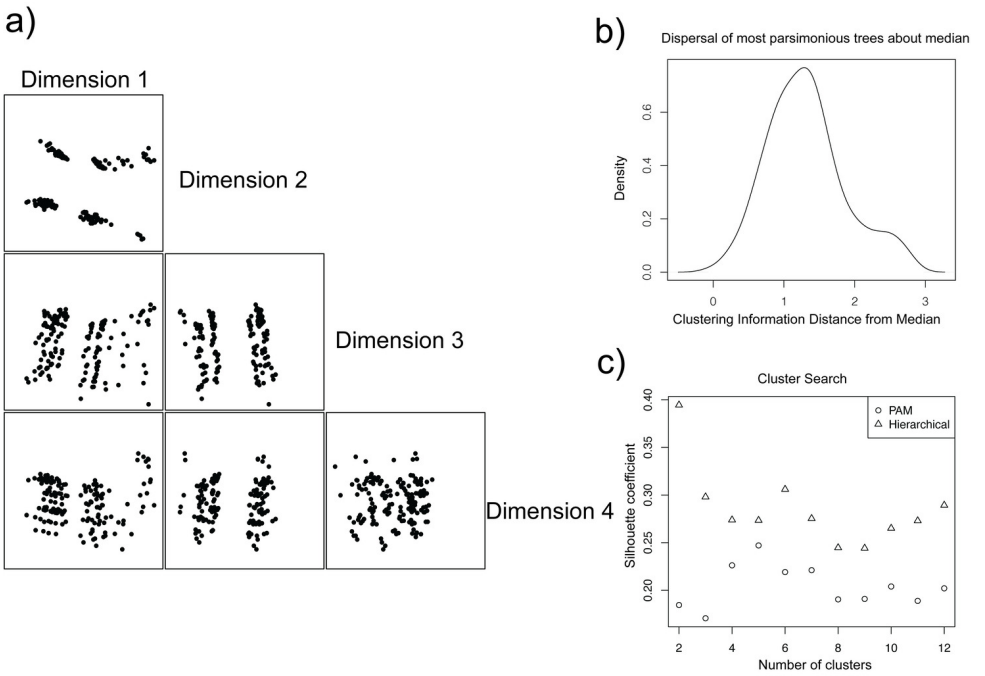

Figure 12. Tree space, dispersal, and cluster search of the restricted parsimony search.

a) Four-dimensional tree space mapping of the most parsimonious trees retained in the restricted search. b) Dispersal of the most parsimonious trees retained in the restricted search. c) Silhouette coefficient of 2-12 clusters identified in the most parsimonious trees retained in the restricted search via PAM and hierarchical clustering via minimax linkage.

the rogue behavior of "*Kalops monophyrum*" arose from conflicts in its character codings rather than missing data. We provide a complete description of each character coding that we changed from the original matrix in the Supplementary Information Part F for future researchers to review and use to avoid a similar rogue taxon problem in their own analyses.

Bayesian search with "Kalops monophryum" recoded as Kalops monophrys

The majority rule consensus tree from our Bayesian analysis of the matrix with "*Kalops monophyrum*" recoded as *Kalops monophrys* is considerably more resolved than our initial Bayesian search (Fig. 14). Devonian "palaeoniscoids" excluding *Cheirolepis* form a paraphyletic grouping at the base of the tree with strong support (estimated posterior probability = 1). *Melanecta* and *Kentuckia* are the first post-Devonian "palaeoniscoids" (Fig. 14a) to branch off, followed by *Woodichthys*. Twelve Mississippian, Pennsylvanian, Permian, and Triassic "palaeoniscoids", including *Tenupiscis*, form an unresolved paraphyletic grouping in the actinopterygian stem (estimated posterior probability = 0.86). The Mississippian *Cyranorhis+Wendyichthys* are resolved as a sister clade to *Actinopterygii* with relatively low support (estimated posterior probability = 0.56; Lund & Poplin, 1997). *Actinopterygii* (Fig. 14b) is inferred as a large polytomy with a series of Mississippian, Pennsylvanian, Permian, and Triassic "palaeoniscoids" and clades containing extant species. The "palaeoniscoids" in *Actinopterygii* include primarily deep bodied species (Eurynotiformes, *Platysomus*, *Aesopichthys*, and a grouping of *Ebenaqua*, *Bobasatrania*, and *Discoserra*. *Birgeria* and *Saurichthys* are resolved within *Actinopterygii*, but the analysis did not find majority support (estimated posterior probability >0.5) for their placement as sister to the pan-acipenseriforms (Fig. 14h) or *Polypteridae+Scanilepiformes* (Fig. 14g). *Australosomus* is also resolved as within *Actinopterygii*. Further, the recoded Bayesian analysis supports the sister group relationship of *Polypteridae+Scanilepiformes* (Fig. 14g; estimated posterior probability = 0.58). *Venusichthys comptus* (Xu & Zhao, 2016) is resolved as the sister taxon to *Neopterygii* (Fig. 14d, estimated posterior probability = 0.73), *Ichthyokentema* (Woodward, 1941) is resolved as the sister taxon to the teleost crown group (Fig. 14e, estimated posterior probability = 0.98), and *Hulettia americana* (Schaeffer & Patterson, 1984) with the dapediids are inferred as the sister clade to the holosteans (Fig. 14f, estimated posterior probability = 0.5).

Discussion

Ray-finned fishes as a case study for the application of tree space in morphological phylogenetics

The apprehension around the choice of incorporating extinct taxa into phylogenetic analyses dates to the inception of phylogenetic systematics (Hennig, 1966). Reluctance to incorporate extinct taxa centers on the idea that the incompleteness of fossil data will almost always prevent it from changing relationships based on analysis of extant groups ("Patterson's Rule"; Grande, 2000; Patterson, 1981), or that missing data will cause extinct terminal taxa to act

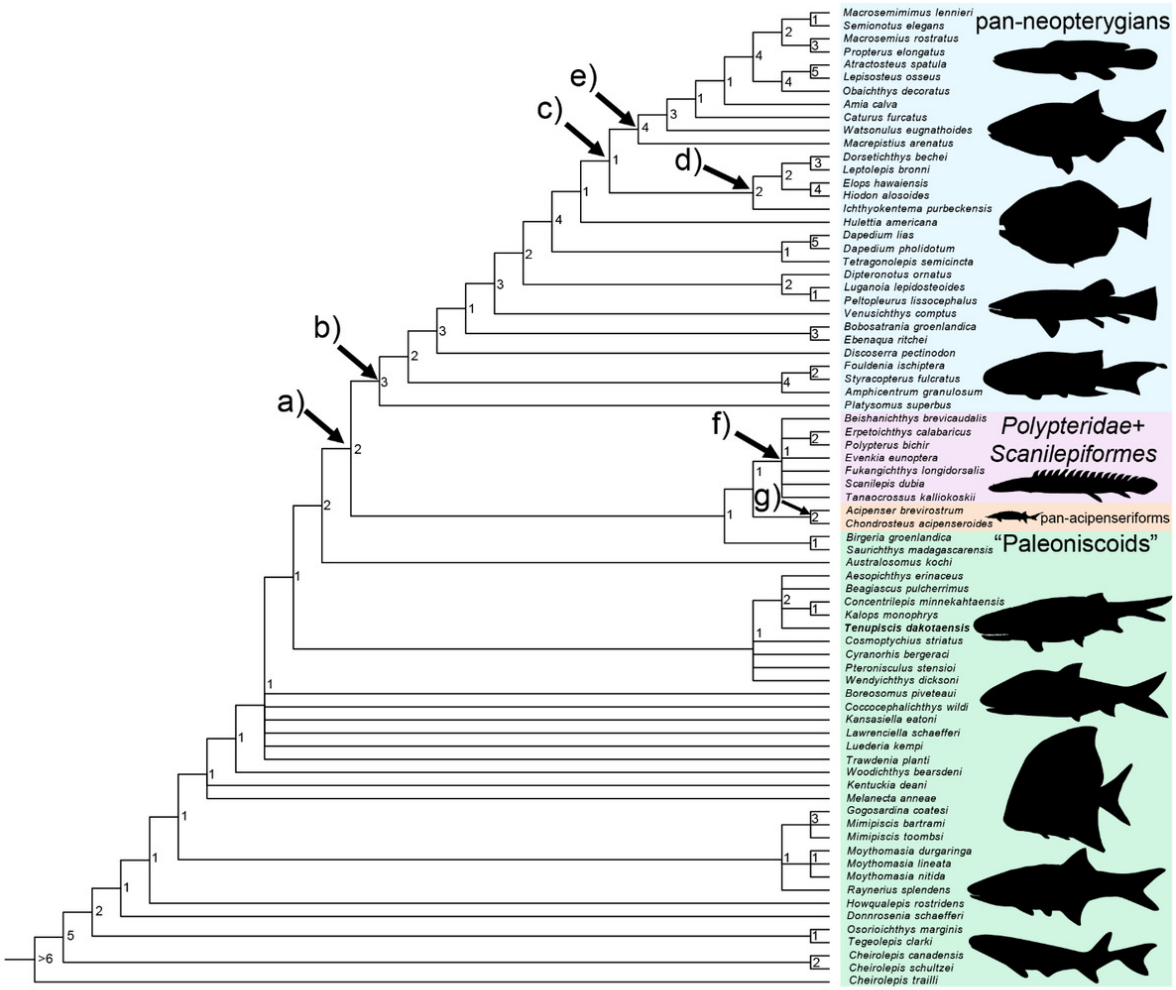

Figure 13. Relationships of *Tenupiscis dakotaensis* gen. et. sp. nov. from a strict consensus of most 2185 most parsimonious trees of length 1096 from a parsimony analysis of 75 taxa (with the rogue taxon "*Kalops monophyrum*" recoded as *Kalops monophrys*) and 222 morphological characters modified from Giles et al. (2017).

Nodes annotated with Bremer decay indices. Consistency index = 0.222 and retention index = 0.606. Abbreviations: a) *Actinopterygii*;b) pan-neopterygians; c) *Neopterygii*; d) pan-teleosteans; e) pan-holosteans; f) *Polypteridae+Scanilepiformes*; g) pan-acipenseriforms. Silhouettes: *Amia*; *Dapedium*; *Hiodon*; *Polypterus*; *Luganoia*; *Fouldenia*; *Acipenser*; *Concentrilepis*; *Boreosomus*; *Platysomus*; *Melanecta*; *Mimipiscus*; *Cheirolepis*.

as "wildcards" (i.e., rogues) and disrupt the consensus results of phylogenetic searches (the "missing data problem"; Kearney, 2002; Kearney & Clark, 2003). However, extinct taxa are useful to reconstructing the relationships of extant taxa (Donoghue et al., 1989; Doyle & Donoghue, 1987; Gauthier et al., 1988; Grande, 2010), do not necessarily act as rogues (Kearney, 2002), and are essential for modeling and analyzing macroevolution (Heath et al., 2014; Koch et al., 2021; Lee & Palci, 2015; Liow et al., 2023; Louca & Pennell, 2020; Slater et al., 2012; Wright et al., 2022). Therefore, the potential problems associated with incorporating extinct taxa must be faced and overcome to meet broader goals in systematic biology.

We found that tree space techniques were essential to overcome the deleterious effect of a rogue taxon in our study of a combined dataset of living and extinct taxa. Although our consensus topologies are informative, they present an incomplete view of the underlying patterns in the phylogenetic results. By design, a consensus topology summarizes many trees as a single topology (Adams, 1972; Margush & McMorris, 1981; Sokal & Rohlf, 1981), meaning that information loss is expected (Wilkinson, 1994). Whereas consensus trees show how sampled topologies agree (Adams, 1972; Margush & McMorris, 1981; Sokal & Rohlf, 1981), tree space methods show how tree search variation is distributed (Bastert et al., 2002; Maddison, 1991; Smith, 2022), illuminating potential sources of consensus uncertainty. The advantage of tree space methods is that they allow us to see the underlying structure of the trees returned by an analysis and incorporate this information when we summarize or make inferences from phylogenetic results.

Tree space methods can reveal hidden, imperfect structure in phylogenetic data that teach us about the evolutionary history of poorly understood groups. The tree space of our initial parsimony search showed that a single rogue

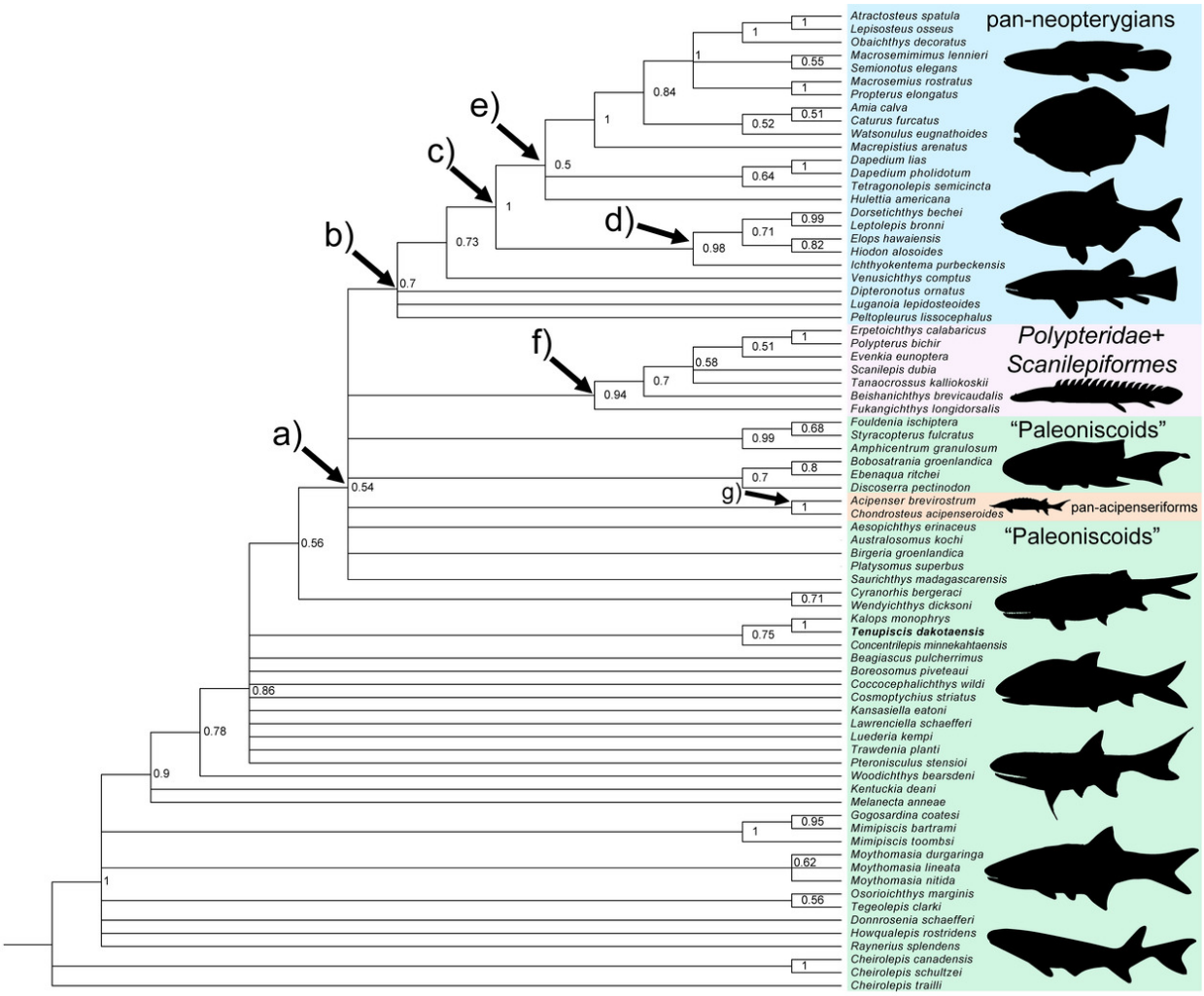

Figure 14. Relationships of *Tenupiscis dakotaensis* gen. et. sp. nov. from a majority rule consensus tree from a Bayesian analysis of 75 taxa (with the rogue taxon "*Kalops monophyrum*" recoded as *Kalops monophrys*) and 222 morphological characters modified from Giles et al. (2017). Phylogenetic hypothesis of actinopterygian interrelationships based on estimated posterior probabilities greater than 0.5 (posterior probability labeled at splits), splits with estimated posterior probability less than 0.5 are condensed to polytomies.

a), *Actinopterygii*. b), pan-neopterygians. c), *Neopterygii*. d), pan-teleosteans. e), pan-holosteans. f), *Polypteridae+Scanilepiformes*. g), pan-acipenseriforms. Silhouettes: *Amia*; *Dapedium*; *Polypterus*; *Fouldenia*; *Acipenser*; *Concentrilepis*; *Boreosomus*; *Melanecta*; *Mimipiscus*; *Cheirolepis*.

taxon divided the most parsimonious trees into two clusters with identical topological variation. This is an empirical example of the theoretical "island problem" described by Maddison (1991), where the strict consensus presents a much less resolved picture than the underlying phylogenetic trees because variation is concentrated between, rather than within islands or clusters (see Maddison, 1991, fig. 7). In our case, the uncertain position of one taxon causes thirteen otherwise resolved terminal taxa to have similar but not identical topological positions. The fourteen-taxon polytomy is therefore a consequence of a single uncertain taxon and a predictable drawback of the strict consensus method (Wilkinson, 1994). We were able to uncover the hidden relationship information by calculating strict consensus topologies for each cluster and conducting separate searches with the rogue taxon either pruned or recoded. Therefore, we can identify and correct for the influence of rogue taxa with tree space methods, revealing reliable phylogenetic patterns in analyses of seemingly poorly resolved groups that provide critical insight into their evolutionary history.

The standard approach in phylogenetic analyses with extinct taxa is to prune suspected rogue taxa to improve the resolution of consensus trees. Rogues are typically identified without a formal rogue taxon search and the initial tree set is often not provided at publication, meaning that other workers cannot verify if the pruned taxa were acting as rogues, or if their pruning was a convenient way to arrive at a more resolved tree. Our results demonstrate the value and importance of carefully examining rogue taxa to determine the source of their behavior. There is no way to know if a rogue arises from incomplete information or conflicting information without examining its scoring, and in the latter case pruning is equivalent to removing a valid

but inconvenient data point to falsely inflate certainty. We strongly recommend that researchers employ rogue taxon search methods (those used here are one of several available techniques, see Aberer et al., 2013; Smith, 2021) and carefully examine any rogues found. Specifically, re-running phylogenetic analyses with rogues pruned versus re-scored shows the influence of the rogue taxa's presence and its original scoring on the initial analysis. With this information in hand, researchers can determine if a rogue is better left out of future searches or if the re-examined version of the taxon should be included. Doing so will, in cases like what is presented here, improve our understanding of the phylogeny and sources of phylogenetic uncertainty in the group of interest.

Tree space techniques can also show when poor resolution arises from a widely dispersed phylogenetic search that is highly uncertain in the position of multiple taxa. The widely dispersed space from our Bayesian analysis is partly a consequence of the aim of the analysis (Wright & Lloyd, 2020). Rather than aiming to find optimal topologies (as in parsimony), the Bayesian analysis samples a set of topologies that includes suboptimal topologies. The summary consensus is based on the frequency of topologies across this broader sample, which is an estimate of the posterior distribution of phylogenetic trees. However, the high number of rogue taxa with low rawImprovement scores in our initial Bayesian search and the wide dispersal of the space verify the uncertainty in the majority rule consensus tree. Simply, our Bayesian search is highly uncertain regarding the relationships of late Paleozoic and early Mesozoic actinopterygians to each other and to extant clades. Verifying that the uncertainty in the consensus is an accurate reflection of the underlying phylogenetic trees, rather than a consequence of clustering, is useful to the progress of phylogenetic research. The Bayesian tree space also highlights the importance of efforts to find more informative characters for late Paleozoic and early Mesozoic actinopterygians, find fossils to fill in missing character data, and examine the design of future Bayesian searches to provide a more-resolved picture.

Every phylogenetic study carries the risk of the strong rogue taxon effects we encountered. We recommend calculating and plotting dispersal as a starting point to check for clustering. Although dispersal is the bare minimum of what tree space has to offer, it is readily interpreted, quick to calculate, and should indicate if the tree sample is sharply divided into clusters. If the tree sample is not sharply divided between two clusters, a single consensus tree will likely provide a reliable summary of the underlying tree space. If an island or clustering problem is apparent in dispersal (or if time allows), we recommend a full study of tree space (as described by Smith, 2022 and conducted here) to search for and identify rogue taxa.

The phylogenetic position of *Tenupiscis* and tracing the roots of the actinopterygian crown into the late Paleozoic

Correcting for the influence of a rogue taxon and running a series of revised parsimony and Bayesian searches shows relationships of *Tenupiscis* and thirteen other taxa that were obscured in our initial analyses. Both our restricted and revised phylogenetic searches indicate that *Tenupiscis* is a member of a long lived (Mississippian–Triassic) actinopterygian stem clade of "palaeoniscoids". Our phylogenetic searches are largely consistent with the series of studies that have modified and expanded the framework of Giles et al. (2017), finding that Mississippian–Triassic "palaeoniscoids" and actinopterygian crown lineages resolve separately from Devonian "palaeoniscoids" and that several lineages of deep bodied Paleozoic taxa branch from the neopterygian stem (Argyriou et al., 2018, 2022; Figueroa et al., 2019, 2021; Giles et al., 2022; Latimer & Giles, 2018; Stack & Gottfried, 2022). The inference that Mississippian–Triassic "palaeoniscoids" include both stem and crown actinopterygians is consistent with molecular evidence that the actinopterygian crown emerged in the Mississippian (Broughton et al., 2013; Near et al., 2012). Our restricted parsimony analysis differs from most previous studies in splitting Mississippian–Triassic stem "palaeoniscoids" into two clades. Previous analyses typically were unable to resolve the relationships of these taxa (Figueroa et al., 2019; Latimer & Giles, 2018; Stack & Gottfried, 2022) or recovered them as a single stem clade with variable internal resolution (Argyriou et al., 2018, 2022; Giles et al., 2017). Our rogue taxon-corrected analyses lend support to the results of Giles et al. (2022), who recovered a similar pattern of multiple clades of "palaeoniscoids" along the actinopterygian stem. Our analyses do not allow for a testing of the tempo of actinopterygian evolution in this interval. However, the fossil-birth death analysis of Giles et al. (2022) on a similar dataset (expanded for Devonian actinopterygians) suggests that the Mississippian clades in our analyses first arose in the Late Devonian, rather than constituting a diversification centered entirely in the Mississippian. Together, these findings suggest that Mississippian-Triassic stem actinopterygians comprise multiple, widespread, and persistent clades that arose by the Mississippian alongside the actinopterygian crown group and persisted into the Triassic.

The emerging picture of the late Paleozoic fossil record shows a diverse actinopterygian assemblage not confined to a morphologically or phylogenetically uniform "palaeoniscoid" wastebasket. Morphological innovation was widespread in late Paleozoic ray-finned fishes, including skeletal adaptations with strikingly similar extant counterparts, including thick palatal tooth plates (Friedman et al., 2019), tricuspid teeth (Poplin & Lund, 2000), elongate rostra (Stack et al., 2020), protrusible jaws (Lund, 2000), a variety of deepened and elongate body forms (Lund & Melton, 1982; Sallan & Coates, 2013), and even regionalization of the vertebral column (Sallan, 2012). Our phylogenetic analyses and the results of Giles et al. (2022) indicate that these traits are spread out amongst multiple clades of stem actinopterygian "palaeoniscoids" and potential early members of the actinopterygian crown group. Further delineating these groups will require much more taxonomic and phylogenetic research. However, we predict that as the evolutionary relationships of the Mississippian–Triassic

actinopterygians are more resolved, ecomorphological diversity will be high among early crown and stem lineages. If this prediction holds, the late Paleozoic will represent the first foray of ray-finned fishes towards the extreme ecological diversity they exhibit today. Therefore, further research on Paleozoic actinopterygians is not only important for singling out the thread of the actinopterygian crown from the vast bundle of early groups. Rather, only by revealing the entire tapestry of this first actinopterygian radiation can we characterize the historical patterns and evolutionary processes that underly extreme species diversity in ray-finned fishes.

Conclusions

We found that *Tenupiscis dakotaensis*, a new genus and species of ray-finned fish from the Lower Permian Minnekahta Limestone (South Dakota, USA), falls within one of two clades of "palaeoniscoid" stem actinopterygians. After correcting for the effect of a rogue taxon, our phylogenetic analyses suggest that multiple stem clades of ray-finned fishes co-existed with potential members of the actinopterygian crown group in the Mississippian and persisted into the Triassic. Gathering more data for groups with poorly understood phylogenies will have limited value without efforts to curb the influence of rogue taxa. Therefore, tree space techniques should become standard practice in phylogenetics because they show the variation underlying consensus topologies, illuminating potential rogue taxa obscuring critical evolutionary patterns.

Funding

Support for this project came from a Michigan State University Distinguished Fellowship, a Michigan State University Department of Earth and Environmental Sciences Alumni Fellowship, a Virginia Tech Geosciences Aubrey & Eula Orange Scholarship, a Virginia Tech Geosciences Heath Robinson-Roy J. Holden Scholarship, a Geological Society of America Graduate Student Research Grant, an American Society of Ichthyologists and Herpetologists Edward C. Raney Fund Award, and a Rodney M. Feldmann Award from the Paleontological Society to Jack Stack.

Acknowledgements

We thank L. Abraczinskas (MSU), Z. Johanson (NHM), E. Bernard (NHM), A. Stroup (FMNH), N. Volden (NMNH), S. Lucas (NMNH), A. Henrici (CMNH), and W. Simpson (FMNH) for providing access to collections. We also thank Martin R Smith (Durham University), Brenen Wynd (Southeastern Louisiana University), Josef Uyeda (Virginia Tech), Sterling Nesbitt (Virginia Tech), and Kate E. Langwig (Virginia Tech) for their assistance with implementing tree space in R. The fossils examined in this research were collected from the ancestral, traditional, and contemporary lands of the Sioux Nation (Dakota, Lakota, Nakota, and Arapaho people) in the Black Hills of South Dakota.

Supporting Information

Data available from the Dryad DigitalRepository: https://doi.org/10.5061/dryad.2bvq83bwf. Extended notes on the methods and additional analysis results are provided in the Supplementary Information document.

Submitted: March 26, 2024 EDT. Accepted: November 22, 2024 EDT. Published: February 17, 2025 EDT.

References

Aberer, A. J., Krompass, D., & Stamatakis, A. (2013). Pruning rogue taxa improves phylogenetic accuracy: An efficient algorithm and webservice. *Systematic Biology*, *62*(1), 162–166. https://doi.org/10.1093/sysbio/sys078

Adams, E. N. (1972). Consensus techniques and the comparison of taxonomic trees. *Systematic Zoology*, *21*(4), 390–397. https://doi.org/10.2307/2412432

Adler, D., & Kelly, S. T. (2022). *vioplot: violin plot* (0.4.0). R package version 0.4.0. https://github.com/TomKellyGenetics/vioplot

Agassiz, L. (1832). Untersuchungen über die fossilen fische der lias-formation. *Neues Jahrbuch für Mineralogie, Geognosie, Geologie und Petrefaktenkunde*, *3*, 139–149.

Aldinger, H. (1937). Permische ganoidfische aus ostgrönland. *Communications of the Natural Research Society of Schaffhausen*.

Ao, S. I., Yip, K., Ng, M., Cheung, D., Fong, P. Y., Melhado, I., & Sham, P. C. (2005). Clustag: Hierarchical clustering and graph methods for selecting tag SNPs. *Bioinformatics*, *21*(8), 1735–1736. https://doi.org/10.1093/bioinformatics/bti201

Argyriou, T., Giles, S., & Friedman, M. (2022). A Permian fish reveals widespread distribution of neopterygian-like jaw suspension. *eLife*, *11*, 1–48. https://doi.org/10.7554/eLife.58433

Argyriou, T., Giles, S., Friedman, M., Romano, C., Kogan, I., & Sánchez-Villagra, M. R. (2018). Internal cranial anatomy of Early Triassic species of †*Saurichthys* (Actinopterygii: †Saurichthyiformes): Implications for the phylogenetic placement of †Saurichthyiforms. *BMC Evolutionary Biology*, *18*, 1–41. https://doi.org/10.1186/s12862-018-1264-4

Arratia, G. (2013). Morphology, taxonomy, and phylogeny of Triassic pholidophorid fishes (Actinopterygii, Teleostei). *Journal of Vertebrate Paleontology*, *33*, 1–138. https://doi.org/10.1080/02724634.2013.835642

Arratia, G., & Cloutier, R. (2004). A new cheirolepidid fish from the middle-upper Devonian. In G. Arratia, M. V. H. Wilson, & R. Cloutier (Eds.), *Recent advances in the origin and early radiation of vertebrates*. Dr. Friedrich Pfeil.

Bastert, O., Rockmore, D., Stadler, P. F., & Tinhofer, G. (2002). Landscapes on spaces of trees. *Applied Mathematics and Computation*, *131*(2–3), 439–459. https://doi.org/10.1016/S0096-3003(01)00164-3

Beer, D., & Beer, A. (2019). *Phylotate: Phylogenies with annotations*.

Behnken, F. H. (1975). Leonardian and Guadalupian (Permian) conodont biostratigraphy in western and southwestern United States. *Journal of Paleontology*, *49*, 284–315. https://www.jstor.org/stable/1303362

Berg, L. S. (1947). *Classification of fishes both recent and fossil*. JW Edwards.

Bien, J., & Tibshirani, R. (2011). Hierarchical clustering with prototypes via minimax linkage. *Journal of the American Statistical Association*, *106*, 1075–1084. https://doi.org/10.1198/jasa.2011.tm10183

Bien, J., & Tibshirani, R. (2022). *Protoclust: Hierarchical clustering with prototypes*.

Boyd, D. W., & Maughan, E. K. (1972). Permian-Triassic boundary in the middle Rocky Mountains. *Bulletin of Canadian Petroleum Geology*, *20*, 676–699. https://doi.org/10.35767/gscpgbull.20.4.676

Braddock, W. A. (1963). Geology of the Jewel Cave SW Quadrangle Custer County, South Dakota. *Geology Survey Bulletin 1063-G*.

Brough, J. (1939). *The Triassic fishes of Besano, Lombardy*. British Museum of Natural History (London).

Broughton, R. E., Betancur-R, R., Li, C., Arratia, G., & Ortí, G. (2013). Multi-locus phylogenetic analysis reveals the pattern and tempo of bony fish evolution. *PLoS Currents*. https://doi.org/10.1371/currents.tol.2ca8041495ffafd0c92756e75247483e

Bürgin, T. (1992). Basal ray-finned fishes (Osteichthyes; Actinopterygii) from the Middle Triassic of Monte San Giorgio (Canton Tessin, Switzerland): Systematic Palaeontology with Notes on functional Morphology and Palaeoecology. *Schweizerische Paläontologische Abhandlungen Mémoires Suisses de Paléontologie*, *114*, 1–164.

Burk, C. A., & Thomas, H. D. (1956). *The Goose Egg Formation (permo-triassic) of eastern Wyoming* (No. 6; The Geological Survey of Wyoming, Report of Investigations). University of Wyoming, Laramie.

Campbell, K., & Phuoc, L. D. (1983). A late Permian actinopterygian fish from Australia. *Palaeontology*, *26*(1), 33–70.

Cantino, P. D., & de Queiroz, K. (2010). *International code of phylogenetic nomenclature (phylocode)*. CRC Press. https://doi.org/10.1201/9780429446320

Choo, B. (2011). Revision of the actinopterygian genus *Mimipiscis* (= *Mimia*) from the upper Devonian Gogo Formation of western Australia and the interrelationships of the early Actinopterygii. *Earth and Environmental Science Transactions of the Royal Society of Edinburgh*, *102*, 77–104. https://doi.org/10.1017/S1755691011011029

Coates, M. I. (1993). New actinopterygian fish from the Namurian Manse Burn Formation of Bearsden, Scotland. *Palaeontology*, *36*, 123–146.

Coates, M. I. (1998). Actinopterygians from the Namurian of Bearsden, Scotland, with comments on early actinopterygian neurocrania. *Zoological Journal of the Linnean Society*, *122*, 27–59. https://doi.org/10.1111/j.1096-3642.1998.tb02524.x

Coates, M. I., & Tietjen, K. (2019). 'This strange little palaeoniscid': A new early actinopterygian genus, and commentary on pectoral fin conditions and function. *Earth and Environmental Science Transactions of The Royal Society of Edinburgh*, *109*(1–2), 15–31. https://doi.org/10.1017/S1755691018000403

Cohen, K. M., Finney, S. C., Gibbard, P. L., & Fan, J. X. (2013). The ICS international chronostratigraphic chart. *Episodes*, *36*, 199–204. https://doi.org/10.18814/epiiugs/2013/v36i3/002

Corn, K. A., Friedman, S. T., Burress, E. D., Martinez, C. M., Larouche, O., Price, S. A., & Wainwright, P. C. (2022). The rise of biting during the Cenozoic fueled reef fish body shape diversification. *Proceedings of the National Academy of Sciences*, *119*(31), e2119828119. https://doi.org/10.1073/pnas.2119828119

de Blainville, H. (1818). Sur les ichthyolites ou les poissons fossiles. *Nouveau Dictionnaire d'Histoire Naturelle, appliquée aux Arts, à l'Agriculture, à l'Economie rurale et domestique, à la Medicine, etc Nouvelle Edition*, *27*, 310–395.

Dierks, N., & Pagnac, D. (2010). Paleozoic fish from the Minnekahta Limestone of the Black Hills. *Proceedings of the South Dakota Academy of Science*, 89.

Donoghue, M. J., Doyle, J. A., Gauthier, J., Kluge, A. G., & Rowe, T. (1989). The importance of fossils in phylogeny reconstruction. *Annual Review of Ecology and Systematics*, *20*, 431–460. https://doi.org/10.1146/annurev.es.20.110189.002243

Dopheide, A. K., & Winniger, N. A. (2008). A Permian stromatolite bioherm in South Dakota: paleoenvironmental implications. *Proceedings of the South Dakota Academy of Science*, *87*, 311–324.

Doyle, J. A., & Donoghue, M. J. (1987). The importance of fossils in elucidating seed plant phylogeny and macroevolution. *Review of Palaeobotany and Palynology*, *50*(1–2), 63–95. https://doi.org/10.1016/0034-6667(87)90040-6

Egerton, P. D. M. G. (1858). On *Chondrosteus*, an extinct genus of the Sturionidae, found in the Lias Formation at Lyme Regis. *Philosophical Transactions of the Royal Society of London*, *148*, 871–885. https://doi.org/10.1098/rstl.1858.0035

Faircloth, B. C., Sorenson, L., Santini, F., & Alfaro, M. E. (2013). A phylogenomic perspective on the radiation of ray-finned fishes based upon targeted sequencing of ultraconserved elements (UCEs). *PloS One*, *8*(6), e65923. https://doi.org/10.1371/journal.pone.0065923

Farris, J. S. (1989). The retention index and the rescaled consistency index. *Cladistics*, *5*(4), 417–419. https://doi.org/10.1111/j.1096-0031.1989.tb00573.x

Figueroa, R. T., Friedman, M., & Gallo, V. (2019). Cranial anatomy of the predatory actinopterygian *Brazilichthys macrognathus* from the Permian (Cisuralian) Pedra de Fogo Formation, Parnaíba Basin, Brazil. *Journal of Vertebrate Paleontology*, *e1639722*, 1–17. https://doi.org/10.1080/02724634.2019.1639722

Figueroa, R. T., Weinschütz, L. C., & Friedman, M. (2021). The oldest Devonian circumpolar ray-finned fish? *Biology Letters*, *17*(3), 20200766. https://doi.org/10.1098/rsbl.2020.0766

Friedman, M. (2015). The early evolution of ray-finned fishes. *Palaeontology*, *58*, 213–228. https://doi.org/10.1111/pala.12150

Friedman, M., Pierce, S. E., Coates, M. I., & Giles, S. (2019). Feeding structures in the ray-finned fish *Eurynotus crenatus* (Actinopterygii: Eurynotiformes): Implications for trophic diversification among Carboniferous actinopterygians. *Earth and Environmental Science Transactions of The Royal Society of Edinburgh*, *109*, 33–47. https://doi.org/10.1017/S1755691018000816

Friedman, M., & Sallan, L. C. (2012). Five hundred million years of extinction and recovery: A Phanerozoic survey of large-scale diversity patterns in fishes. *Palaeontology*, *55*, 707–742. https://doi.org/10.1111/j.1475-4983.2012.01165.x

Gardiner, B. G. (1984). The relationships of the palaeoniscid fishes, a review based on new specimens of *Mimia* and *Moythomasia* from the Upper Devonian of western Australia. *Bulletin of the British Museum (Natural History), Geology Series*, *37*, 173–428.

Gardiner, B. G., & Bartram, A. W. H. (1977). The homologies of ventral cranial fissures in osteichthyans. In S. M. Andrews, R. S. Miles, & A. D. Walker (Eds.), *Problems in vertebrate evolution* (pp. 227–245). Academic Press.

Gardiner, B. G., & Schaeffer, B. (1989). Interrelationships of lower actinopterygian fishes. *Zoological Journal of the Linnean Society*, *97*, 135–187. https://doi.org/10.1111/j.1096-3642.1989.tb00550.x

Gauthier, J., Kluge, A. G., & Rowe, T. (1988). Amniote phylogeny and the importance of fossils. *Cladistics*, *4*(2), 105–209. https://doi.org/10.1111/j.1096-0031.1988.tb00514.x

Gelman, A., & Rubin, D. B. (1992). Inference from iterative simulation using multiple sequences. *Statistical Science*, *7*(4), 457–472. https://doi.org/10.1214/ss/1177011136

Giles, S., Feilich, K., Warnock, R. C., Pierce, S. E., & Friedman, M. (2022). A late Devonian actinopterygian suggests high lineage survivorship across the end-Devonian mass extinction. *Nature Ecology & Evolution*, *7*(1), 10–19. https://doi.org/10.1038/s41559-022-01919-4

Giles, S., Xu, G.-H., Near, T. J., & Friedman, M. (2017). Early members of 'living fossil' lineage imply later origin of modern ray-finned fishes. *Nature*, *549*(7671), 265–268. https://doi.org/10.1038/nature23654

Goloboff, P. A., & Catalano, S. A. (2016). TNT version 1.5, including a full implementation of phylogenetic morphometrics. *Cladistics*, *32*(3), 221–238. https://doi.org/10.1111/cla.12160

Goloboff, P. A., Farris, J. S., & Nixon, K. C. (2008). TNT, a free program for phylogenetic analysis. *Cladistics*, *24*(5), 774–786. https://doi.org/10.1111/j.1096-0031.2008.00217.x

Gradstein, F. M., Ogg, J. G., Schmitz, M. D., & Ogg, G. M. (2012). *The Geologic Time Scale 2012*. Elsevier. https://doi.org/10.1127/0078-0421/2012/0020

Grande, L. (2000). Fossils, phylogeny, and Patterson's rule. Colin Patterson (1933–1998): a celebration of his life. *Special Issue No 2, The Linnean Society of London*, Article 2.

Grande, L. (2010). An empirical synthetic pattern study of gars (Lepisosteiformes) and closely related species, based mostly on skeletal anatomy. The resurrection of Holostei. *Ichthyology & Herpetology*, *10*(2A), 1–871.

Grande, L., & Bemis, W. E. (1991). Osteology and phylogenetic relationships of fossil and recent paddlefishes (Polyodontidae) with comments on the interrelationships of Acipenseriformes. *Journal of Vertebrate Paleontology*, *11*(S1), 1–121. https://doi.org/10.1080/02724634.1991.10011424

Grande, L., & Bemis, W. E. (1998). A comprehensive phylogenetic study of amiid fishes (Amiidae) based on comparative skeletal anatomy. An empirical search for interconnected patterns of natural history. *Journal of Vertebrate Paleontology*, *18*(sup1), 1–696. https://doi.org/10.1080/02724634.1998.10011114

Gregory, W. K. (1932). Some strange teleost skulls and their derivation from normal forms. *Copeia*, *1932*(2), 53–60. https://doi.org/10.2307/1435883

Hamel, M.-H., & Poplin, C. (2008). The braincase anatomy of *Lawrenciella schaefferi*, actinopterygian from the Upper Carboniferous of Kansas (USA). *Journal of Vertebrate Paleontology*, *28*(4), 989–1006. https://doi.org/10.1671/0272-4634-28.4.989

Heath, T. A., Huelsenbeck, J. P., & Stadler, T. (2014). The fossilized birth–death process for coherent calibration of divergence-time estimates. *Proceedings of the National Academy of Sciences*, *111*(29), E2957–E2966. https://doi.org/10.1073/pnas.1319091111

Hendy, M. D., Steel, M. A., Penny, D., & Henderson, I. M. (1988). Families of trees and consensus. In H. H. Bock (Ed.), *Classification and related methods of data analysis*. Elsevier Science Publishers.

Hennig, W. (1966). *Phylogenetic systematics* (D. D. Davis & R. Zangerl, Trans.). University of Illinois Press.

Hillis, D. M., Heath, T. A., & John, K. S. (2005). Analysis and visualization of tree space. *Systematic Biology*, *54*(3), 471–482. https://doi.org/10.1080/10635150590946961

Hilton, E. J., Grande, L., & Bemis, W. E. (2011). Skeletal anatomy of the shortnose sturgeon, *Acipenser brevirostrum* Lesueur, 1818, and the systematics of sturgeons (Acipenseriformes, Acipenseridae). *Fieldiana Life and Earth Sciences*, *3*(3), 1–168. https://doi.org/10.3158/2158-5520-3.1.1

Houle, D., Govindaraju, D. R., & Omholt, S. (2010). Phenomics: The next challenge. *Nature Reviews Genetics*, *11*(12), 855–866. https://doi.org/10.1038/nrg2897

Hurley, I. A., Mueller, R. L., Dunn, K. A., Schmidt, E. J., Friedman, M., Ho, R. K., Prince, V. E., Yang, Z., Thomas, M. G., & Coates, M. I. (2007). A new time-scale for ray-finned fish evolution. *Proceedings of the Royal Society B: Biological Sciences*, *274*(1609), 489–498. https://doi.org/10.1098/rspb.2006.3749

Hussakof, L. (1916). Note on a palaeoniscoid fish from a Permian formation in South Dakota. *American Journal of Science*, *25*, 347–350. https://doi.org/10.2475/ajs.s4-41.244.347

Inden, R. F., & Coalson, E. B. (1996). Phosphoria Formation (Permian) cycles in the Bighorn Basin, Wyoming, with emphasis on the Ervay Member. In M. W. Longman (Ed.), *Paleozoic systems of the Rocky Mountain Region*. The Rocky Mountain Section of the Society for Sedimentary Geology.

Kaski, S., Nikkilä, J., Oja, M., Venna, J., Törönen, P., & Castrén, E. (2003). Trustworthiness and metrics in visualizing similarity of gene expression. *BMC Bioinformatics*, *4*, 1–13. https://doi.org/10.1186/1471-2105-4-48

Kaufman, L., & Rousseeuw, P. J. (1990). *Partitioning around medoids (program PAM). Finding groups in data: An introduction to cluster analysis*. John Wiley & Sons, Ltd.

Kearney, M. (2002). Fragmentary taxa, missing data, and ambiguity: Mistaken assumptions and conclusions. *Systematic Biology*, *51*(2), 369–381. https://doi.org/10.1080/10635150601115624

Kearney, M., & Clark, J. M. (2003). Problems due to missing data in phylogenetic analyses including fossils: A critical review. *Journal of Vertebrate Paleontology*, *23*, 263–274. https://doi.org/10.1671/0272-4634(2003)023

Kluge, A. G., & Farris, J. S. (1969). Quantitative phyletics and the evolution of Anurans. *Systematic Biology*, *18*(1), 1–32. https://doi.org/10.1093/sysbio/18.1.1

Koch, N. M., Garwood, R. J., & Parry, L. A. (2021). Fossils improve phylogenetic analyses of morphological characters. *Proceedings of the Royal Society B*, *288*(1950), 20210044. https://doi.org/10.1098/rspb.2021.0044

Kocsis, Á. T., & Raja, N. B. (2020). *Chronosphere: Earth system history variables*. https://doi.org/10.32614/CRAN.package.chronosphere

Lacépède, B. G. (1803). *Histoire naturelle des poissons*. Plasson. https://doi.org/10.5962/bhl.title.6882

Latimer, A. E., & Giles, S. (2018). A giant dapediid from the Late Triassic of Switzerland and insights into neopterygian phylogeny. *Royal Society Open Science*, *5*(180497), 1–19. https://doi.org/10.1098/rsos.180497

Le Sueur, C. A. (1818). Description of several species of chondropterigious fishes of North America. *Transactions of the American Philosophical Society*, *1*, 383–394. https://doi.org/10.2307/1004927

Lee, M. S., & Palci, A. (2015). Morphological phylogenetics in the genomic age. *Current Biology*, *25*(19), R922–R929. https://doi.org/10.1016/j.cub.2015.07.009

Lewis, P. O. (2001). A likelihood approach to estimating phylogeny from discrete morphological character data. *Systematic Biology*, *50*(6), 913–925. https://doi.org/10.1080/106351501753462876

Linnaeus, C. (1766). *Systema naturae. Editio duodecima, reformata* (pp. 1–532). Laurientii Salvii, Holmiae, Stockholm.

Liow, L. H., Uyeda, J., & Hunt, G. (2023). Cross-disciplinary information for understanding macroevolution. *Trends in Ecology & Evolution*, *38*(3), 250–260. https://doi.org/10.1016/j.tree.2022.10.013

Louca, S., & Pennell, M. W. (2020). Extant timetrees are consistent with a myriad of diversification histories. *Nature*, *580*(7804), 502–505. https://doi.org/10.1038/s41586-020-2176-1

Lund, R. (2000). The new actinopterygian order Guildayichthyiformes from the lower Carboniferous of Montana (USA). *Geodiversitas*, *22*(2), 171–206.

Lund, R., & Melton, W. (1982). *Paratarrasius hibbardi* new genus and species (Actinopterygii, Tarrasiiformes) from the Namurian Bear Gulch Limestone of Montana, USA. *Palaeontology*, *25*, 485–498.

Lund, R., & Poplin, C. (1997). The rhadinichthyids (paleoniscoid actinopterygians) from the Bear Gulch Limestone of Montana (USA, Lower Carboniferous). *Journal of Vertebrate Paleontology*, *17*(3), 466–486. https://doi.org/10.1080/02724634.1997.10010996

Lund, R., & Poplin, C. (2002). Cladistic analysis of the relationships of the tarrasiids (lower Carboniferous actinopterygians). *Journal of Vertebrate Paleontology*, *22*(3), 480–486. https://doi.org/10.1671/0272-4634(2002)022

Maddison, D. R. (1991). The discovery and importance of multiple islands of most parsimonious trees. *Systematic Zoology*, *40*(3), 315–328. https://doi.org/10.1093/sysbio/40.3.315

Maechler, M., Rousseeuw, P., Struyf, A., Hubert, M., & Hornik, K. (2022). *Cluster: Cluster analysis basics and extensions* (2.1.3). https://CRAN.R-project.org/package=cluster

Margush, T., & McMorris, F. R. (1981). Consensus n-trees. *Bulletin of Mathematical Biology*, *43*(2), 239–244. https://doi.org/10.1007/BF02459446

Maughan, E. K. (1994). Phosphoria Formation (Permian) and its resource significance in the western interior, USA. In A. F. Embry, B. Beauchamp, & D. J. Glass (Eds.), *Pangea: Global environments and resources* (pp. 479–495). Canadian Society of Petroleum Geologists.

Mickle, K. E. (2017). The lower actinopterygian fauna from the lower Carboniferous Albert Shale Formation of New Brunswick, Canada–a review of previously described taxa and a description of a new genus and species. *Fossil Record*, *20*(1), 47–67. https://doi.org/10.5194/fr-20-47-2017

Mickle, K. E., Lund, R., & Grogan, E. D. (2009). Three new palaeoniscoid fishes from the Bear Gulch Limestone (Serpukhovian, Mississippian) of Montana (USA) and the relationships of lower actinopterygians. *Geodiversitas*, *31*(3), 623–668. https://doi.org/10.5252/g2009n3a6

Moore, J. A., & Near, T. J. (2020). Pan-Actinopterygii. In K. D. Queiroz, P. D. Cantino, & J. A. Gauthier (Eds.), *Phylonyms: a companion to the PhyloCode* (pp. 695–699). Taylor & Francis Group. https://doi.org/10.1201/9780429446276

Moy-Thomas, J. A., & Bradley Dyne, M. (1938). XVII.—the actinopterygian fishes from the lower Carboniferous of Glencartholm, Eskdale, Dumfriesshire. *Earth and Environmental Science Transactions of The Royal Society of Edinburgh*, *59*, 437–480. https://doi.org/10.1017/S0080456800009170

Murtagh, F. (1983). A survey of recent advances in hierarchical clustering algorithms. *The Computer Journal*, *26*(4), 354–359. https://doi.org/10.1093/comjnl/26.4.354

Near, T. J., Eytan, R. I., Dornburg, A., Kuhn, K. L., Moore, J., Davis, M. P., Wainwright, P. C., Friedman, M., & Smith, W. L. (2012). Resolution of ray-finned fish phylogeny and timing of diversification. *PNAS*, *109*, 13698–13703. https://doi.org/10.1073/pnas.1206625109

Near, T. J., & Thacker, C. E. (2024). Phylogenetic classification of living and fossil ray-finned fishes (Actinopterygii). *Bulletin of the Peabody Museum of Natural History*, *65*(1), 3–302. https://doi.org/10.3374/014.065.0101

Nelson, J. S., Grande, T. C., & Wilson, M. V. (2016). *Fishes of the world*. John Wiley & Sons. https://doi.org/10.1002/9781119174844

Nielsen, E. (1942). Studies on Triassic fishes from east Greenland 1. *Glaucolepis* and *Boreosomus*. *Palaeozoologica Groenlandica*, *1*(1), 1–403.

Nixon, K. C., & Carpenter, J. M. (1996). On consensus, collapsibility, and clade concordance. *Cladistics*, *12*(4), 305–321. https://doi.org/10.1111/j.1096-0031.1996.tb00017.x

Nixon, K. C., & Wheeler, Q. D. (1992). Extinction and the origin of species. In M. J. Novacek & Q. D. Wheeler (Eds.), *Extinction and phylogeny* (p. 143). Colombia University Press.

Paradis, E., & Schliep, K. (2019). Ape 5.0: An environment for modern phylogenetics and evolutionary analyses in R. *Bioinformatics*, *35*, 526–528. https://doi.org/10.1093/bioinformatics/bty633

Patterson, C. (1981). Significance of fossils in determining evolutionary relationships. *Annual Review of Ecology and Systematics*, *12*(1), 195–223. https://doi.org/10.1146/annurev.es.12.110181.001211

Patterson, C. (1982). Morphology and interrelationships of primitive actinopterygian fishes. *American Zoologist*, *22*, 241–295. https://doi.org/10.1093/icb/22.2.241

Piper, D. Z., & Link, P. K. (2002). An upwelling model for the Phosphoria sea: a Permian, ocean-margin sea in the northwest United States. *AAPG Bulletin*, *86*, 1217–1235. https://doi.org/10.1306/61EEDC60-173E-11D7-8645000102C1865D

Piveteau, J. (1945). Paléontologie de Madagascar xxv.—les poissons du trias inférieur, la familledes saurichthyidés. *Annales de Paléontologie*, *31*, 79–89.

Poplin, C. (1974). *Étude de quelques paléoniscidés pennsylvaniens du Kansas*. Cahiers de Paléontologie (Section Vertébrés).

Poplin, C., & Lund, R. (2000). Two new deep-bodied paleoniscoid actinopterygians from Bear Gulch (Montana, USA, lower Carboniferous). *Journal of Vertebrate Paleontology*, *20*, 428–449. https://doi.org/10.1671/0272-4634(2000)020

Poplin, C., & Lund, R. (2002). Two Carboniferous fine-eyed palaeoniscoids (Pisces, Actinopterygii) from Bear Gulch (USA). *Journal of Paleontology*, *76*, 1014–1028. https://doi.org/10.1666/0022-3360(2002)076

R Core Team. (2021). *R: A language and environment for statistical computing*. R Foundation for Statistical Computing. https://www.R-project.org/

Rafinesque, C. S. (1819). Prodrome de 70 nouveaux genres d'animaux decouvert dans tinterieur des etats-unis d'amerique durant i'annee 1818. *Journal de Physique*, *88*, 417–429.

Rambaut, A. (2018). *Figtree tree figure drawing tool version 1.4.4*. https://github.com/rambaut/figtree/releases

Rambaut, A., Drummond, A. J., Xie, D., Baele, G., & Suchard, M. A. (2018). Posterior summarization in Bayesian phylogenetics using Tracer 1.7. *Systematic Biology*, *67*(5), 901–904. https://doi.org/10.1093/sysbio/syy032

Regan, C. T. (1909). A revision of the fishes of the genus *Elops*. *Annals and Magazine of Natural History*, *3*(13), 37–40. https://doi.org/10.1080/00222930908692543

Regan, C. T. (1923). The skeleton of *Lepidosteus*, with remarks on the origin and evolution of the lower neopterygian fishes. *Proceedings of the Zoological Society London*, *93*, 445–461. https://doi.org/10.1111/j.1096-3642.1923.tb02191.x

Revell, L. J. (2012). Phytools: An R package for phylogenetic comparative biology (and other things). *Methods in Ecology and Evolution*, *2*, 217–223. https://doi.org/10.1111/j.2041-210X.2011.00169.x

Ripley, B. D. (1987). *Stochastic simulation*. John Wiley & Sons. https://doi.org/10.1002/9780470316726

Romano, C. (2021). A hiatus obscures the early evolution of modern lineages of bony fishes. *Frontiers in Earth Science*, *8*, 618853. https://doi.org/10.3389/feart.2020.618853

Ronquist, F., Teslenko, M., Van Der Mark, P., Ayres, D. L., Darling, A., Höhna, S., Larget, B., Liu, L., Suchard, M. A., & Huelsenbeck, J. P. (2012). MrBayes 3.2: Efficient bayesian phylogenetic inference and model choice across a large model space. *Systematic Biology*, *61*(3), 539–542. https://doi.org/10.1093/sysbio/sys029

Rowe, T. (2004). Chordate phylogeny and development. In J. Cracraft & M. J. Donoghue (Eds.), *Assembling the tree of life* (pp. 384–409). Oxford University Press. https://doi.org/10.1093/oso/9780195172348.003.0024

Sallan, L. C. (2012). Tetrapod-like axial regionalization in an early ray-finned fish. *Proceedings of the Royal Society B: Biological Sciences*, *279*(1741), 3264–3271. https://doi.org/10.1098/rspb.2012.0784

Sallan, L. C. (2014). Major issues in the origins of ray-finned fish (Actinopterygii) biodiversity. *Biological Reviews*, *89*(4), 950–971. https://doi.org/10.1111/brv.12086

Sallan, L. C., & Coates, M. I. (2013). Styracopterid (Actinopterygii) ontogeny and the multiple origins of post-Hangenberg deep-bodied fishes: Early Carboniferous Styracopterid fishes. *Zoological Journal of the Linnean Society*, *169*, 156–199. https://doi.org/10.1111/zoj.12054

Sanderson, M. J., & Shaffer, H. B. (2002). Troubleshooting molecular phylogenetic analyses. *Annual Review of Ecology and Systematics*, *33*, 49–72. https://doi.org/10.1146/annurev.ecolsys.33.010802.150509

Schaeffer, B., & Dalquest, W. W. (1978). A palaeonisciform braincase from the Permian of Texas, with comments on cranial fissures and the posterior myodome. *American Museum Novitates*, *2658*, 1–15. http://hdl.handle.net/2246/5327

Schaeffer, B., & Patterson, C. (1984). Jurassic fishes from the western United States, with comments on Jurassic fish distribution. *American Museum Novitates*, *2796*. https://www.biodiversitylibrary.org/item/317403

Schubert, E., & Rousseeuw, P. J. (2021). Fast and eager k-medoids clustering: O(k) runtime improvement of the PAM, CLARA, and CLARANS algorithms. *Information Systems*, *101*, 101804. https://doi.org/10.1016/j.is.2021.101804

Schultze, H.-P. (2016). Scales, enamel, cosmine, ganoine, and early osteichthyans. *Comptes Rendus Palevol*, *15*(1–2), 83–102. https://doi.org/10.1016/j.crpv.2015.04.001

Silva, A. S., & Wilkinson, M. (2021). On defining and finding islands of trees and mitigating large island bias. *Systematic Biology*, *70*(6), 1282–1294. https://doi.org/10.1093/sysbio/syab015

Slater, G. J., Harmon, L. J., & Alfaro, M. E. (2012). Integrating fossils with molecular phylogenies improves inference of trait evolution. *Evolution*, *66*(12), 3931–3944. https://doi.org/10.1111/j.1558-5646.2012.01723.x

Smith, M. R. (2019). *Treetools: Create, modify and analyse phylogenetic trees*. Comprehensive R Archive Network. https://doi.org/10.32614/CRAN.package.TreeTools

Smith, M. R. (2020a). Information theoretic generalized Robinson–Foulds metrics for comparing phylogenetic trees. *Bioinformatics*, *36*(20), 5007–5013. https://doi.org/10.1093/bioinformatics/btaa614

Smith, M. R. (2020b). *Treedist: Distances between phylogenetic trees* (2.4.0). R package version 2.4.0. https://doi.org/10.32614/CRAN.package.TreeDist

Smith, M. R. (2021). Using information theory to detect rogue taxa and improve consensus trees. *Systematic Biology*, *0*, 1–7. https://doi.org/10.1093/sysbio/syab099

Smith, M. R. (2022). Robust analysis of phylogenetic tree space. *Systematic Biology*, *0*(syab099), 1–16. https://doi.org/10.1093/sysbio/syab100

Sokal, R. R., & Rohlf, F. J. (1981). Taxonomic congruence in the Leptopodomorpha re-examined. *Systematic Zoology*, *30*(3), 309–325. https://doi.org/10.2307/2413252

Stack, J., & Gottfried, M. D. (2022). A new, exceptionally well-preserved Permian actinopterygian fish from the Minnekahta Limestone of South Dakota, USA. *Journal of Systematic Palaeontology*, *19*, 1271–1302. https://doi.org/10.1080/14772019.2022.2036837

Stack, J., Hodnett, J.-P., Lucas, S. G., & Sallan, L. C. (2020). *Tanyrhinichthys mcallisteri*, a long-rostrumed Pennsylvanian ray-finned fish (Actinopterygii) and the simultaneous appearance of novel ecomorphologies in late Palaeozoic fishes. *Zoological Journal of the Linnean Society*, *191*(2), 347–374. https://doi.org/10.1093/zoolinnean/zlaa044

Stensiö, E. A. (1932). Triassic fishes from east Greenland. *Meddelelser Om Grønland*, *83*, 125–164.

Summers, A. P. (2018). How and why to scan all the vertebrates-open access data as a transformative tool. *The FASEB Journal*, *32*, 84.8384.83. https://doi.org/10.1096/fasebj.2018.32.1_supplement.84.3

Swofford, D. L. (2003). *PAUP*. Phylogenetic analysis using parsimony (* and other methods)*. Sinauer Associates.

Szabó, M., & Pálfy, J. (2020). *Dapedium* sp. from the Toarcian (Lower Jurassic) Úrkút Manganese Ore Formation (Bakony Mts., Hungary) and an overview of diversity of dapediiform fishes. *Palaeobiodiversity and Palaeoenvironments*, *100*, 179–195. https://doi.org/10.1007/s12549-019-00390-7

Traquair, R. H. (1881). Report on fossil fishes collected by the geological survey of Scotland in Eskdale and Liddesdale. Part i: Ganoidei. *Transactions of the Royal Society of Edinburgh*, *30*, 15–71. https://doi.org/10.1017/S0080456800028970

Traquair, R. H. (1911). The ganoid fishes of the British carboniferous formations. Part V. *Palaeontographical Society (Monographs)*, *64*, 123–158. https://doi.org/10.1080/02693445.1911.12035550

Trautwein, M. D., Wiegmann, B. M., & Yeates, D. K. (2011). Overcoming the effects of rogue taxa: Evolutionary relationships of the bee flies. *PLoS Currents*, *3*.

Venna, J., & Kaski, S. (2001). Neighborhood preservation in nonlinear projection methods: An experimental study. In G. Dorffner, H. Bischof, & K. Hornik (Eds.), *Artificial neural networks — ICANN 2001* (pp. 485–492). Springer. https://doi.org/10.1007/3-540-44668-0_68

Wardlaw, B. R., & Collinson, J. W. (1986). Paleontology and deposition of the Phosphoria Formation. *Contributions to Geology, University of Wyoming*, *24*, 107–142.

Watson, D. M. S. (1925). The structure of certain palaeoniscoids and the relationships of that group with other bony fish. *Proceedings of the Zoological Society of London*, 815–870. https://doi.org/10.1111/j.1469-7998.1925.tb07107.x

Watson, D. M. S. (1928). On some points in the structure of palæoniscid and allied fish. *Proceedings of the Zoological Society of London*, *IV*. https://doi.org/10.1111/j.1469-7998.1928.tb07140.x

Whalen, M. T. (1996). Facies architecture of the Permian Park City Formation, Utah and Wyoming: Implications for the paleogeography and oceanographic setting of western Pangea. In M. W. Longman & M. D. Sonnenfield (Eds.), *Paleozoic systems of the Rocky Mountain region*. Rocky Mountain Section SEPM.

Whiteaves, J. F. (1881). On some remarkable fossil fishes from the Devonian rocks of Scaumenac Bay, in the province of Quebec. *Journal of Natural History*, *8*(44), 159–162. https://doi.org/10.1080/00222938109487434

Wilgus, C. K., & Holser, W. T. (1984). Marine and nonmarine salts of western interior, United States. *AAPG Bulletin*, *68*, 765–767. https://doi.org/10.1306/AD461386-16F7-11D7-8645000102C1865D

Wilkinson, M. (1994). Common cladistic information and its consensus representation: Reduced Adams and reduced cladistic consensus trees and profiles. *Systematic Biology*, *43*(3), 343–368. https://doi.org/10.1093/sysbio/43.3.343

Wilkinson, M. (2003). Missing entries and multiple trees: Instability, relationships, and support in parsimony analysis. *Journal of Vertebrate Paleontology*, *23*, 311–323. https://doi.org/10.1671/0272-4634(2003)023

Wilkinson, M., & Benton, M. J. (1995). Missing data and rhynchosaur phylogeny. *Historical Biology*, *10*(2), 137–150. https://doi.org/10.1080/10292389509380517

Woodward, A. S. (1941). VIII.—The Mesozoic ganoid fishes of the genus *Pholidophorus* Agassiz. *Journal of Natural History*, *8*(44), 88–91. https://doi.org/10.1080/03745481.1941.9727955

Wright, A. M., Bapst, D. W., Barido-Sottani, J., & Warnock, R. C. (2022). Integrating fossil observations into phylogenetics using the fossilized birth–death model. *Annual Review of Ecology, Evolution, and Systematics*, *53*, 251–273. https://doi.org/10.1146/annurev-ecolsys-102220-030855

Wright, A. M., & Lloyd, G. T. (2020). Bayesian analyses in phylogenetic palaeontology: interpreting the posterior sample. *Palaeontology*, 1–10. https://doi.org/10.1111/pala.12500

Xu, G.-H. (2020). A new species of *Luganoia* (Luganoiidae, Neopterygii) from the Middle Triassic Xingyi biota, Guizhou, China. *Vertebrata PalAsiatica*, *58*(4), 1–16. https://doi.org/10.19615/j.cnki.1000-3118.200624

Xu, G.-H., & Zhao, L.-J. (2016). A middle Triassic stem-neopterygian fish from China shows remarkable secondary sexual characteristics. *Science Bulletin*, *61*, 338–344. https://doi.org/10.1007/s11434-016-1189-5

Young, J. (1866). On the affinities of *Platysomus* and allied genera. *Quarterly Journal of the Geological Society*, *22*(1–2), 301–317. https://doi.org/10.1144/GSL.JGS.1866.022.01-02.22